Supporting Information

For

Photo-induced nitroxyl anion/HNO release from a nitrosyl complex of Mn(II)-porphyrinate

Shankhadeep Saha, Sayani Maity, Bapan Samanta, Riya Ghosh, Kalishankar Bhattacharyya, Biplab Mondal*

Department of Chemistry, Indian Institute of Technology Guwahati, Assam – 781039, India.

Email: biplab@iitg.ac.in; Phone : (+)91-361-258-2317; Fax: (+)91-361-258-2339

Table of contents

Experimental Section

Materials and Methods

All experiments, unless otherwise specified, were done under Argon atmosphere using standard Schlenk techniques on Schlenk line. All chemicals used were of reagent grade, purchased from commercially available sources and no purification was done unless mentioned. Methanol was distilled using Mg-turnings and Iodine. Tetrahydrofurane (THF) was dried by distillation with sodium and benzophenone. Dichloromethane was purified by passing through a basic alumina column, then storing over calcium hydride for overnight and followed by distillation under inert atmosphere (N_2). All the solvents were stored over molecular sieve (4 Å) for at least two days under Argon before using. Molecular sieves were kept at 200 °C for 24 h for activation and cooled under vacuum. Solvents and solutions were deoxygenated by applying consecutive vacuum/Argon purge cycles. All the reactions were performed under inert atmosphere except mentioned differently.

UV–visible spectra were taken on an Agilent Cary 8454 spectrophotometer. FT-IR spectra were recorded as KBr pellets or in a KBr cell using a PerkinElmer spectrophotometer. ^{1}H, ^{13}C, and ^{31}P NMR studies were done in 400 and 500 MHz Varian FT-NMR spectrophotometers. Fluorescence spectra were recorded on Fluoromax + spectrophotometer. X-band EPR spectra were recorded on a JES-FA200 EPR spectrophotometer with microwave power, 0.998 mW; microwave frequency, 9.14 GHz; and modulation amplitude, 2. Gas chromatograms were obtained on PerkinElmer Clarus® 590.

Single crystals were grown from dichloromethane-methanol solutions using the slow evaporation technique. The intensity data were collected using a Bruker SMART APEX-IV CCD diffractometer, equipped with a fine focus 1.75 kW sealed tube Mo Kα radiation (λ = 0.71073 Å), with increasing ω (width of 0.3° per frame) at a scan speed of 3 s/frame. The

SMART software was used for data acquisition. Data integration and reduction were undertaken with SAINT and XPREP software.[1] Structures were solved by direct methods using SHELXS-2016 and refined with full-matrix least-squares on F^2 using SHELXL-2016/6.[2a] Structural illustrations were drawn with ORTEP-3 for Windows.[2b]

Computational Details:

All the computational calculations are carried out using the Gaussian 16 suite of programs.[3] Geometries of the NO-bound Mn-Porphyrin structure was fully optimized using the B3LYP/6-31+G(D,P) level of theory.[4,5] Vibrational frequency analyses were conducted on these optimized structures to ensure no imaginary frequencies were present.

Syntheses

5,10,15,20-tetrakis(3,4,5-trimethoxyphenyl) porphyrin (H_2TTMPP):

The trimethoxyphenyl substituted porphyrin was synthesized following Alder and Longo methods. To a 250 mL round bottom flask equipped with a magnetic stir-bar, equimolar amount of 3,4,5-trimethoxybenzaldehyde (3.92g, 20 mmol) and freshly distilled pyrrole (1.34g, 20 mmol) was added followed by 75 mL of propionic acid. The mixture was refluxed for 2 h. The reaction mixture was left overnight at room temperature upon which purple crystalline solid was precipitated. It was filtered and washed with hot water followed by hexane. Shiny purple crystals of pure H_2TTMPP obtained. Yield ~ 24% (1.17g). Elemental analyses for $C_{56}H_{54}N_4O_{12}$ Calculated (%): C, 68.98; H, 5.58; N, 5.75. found (%): C, 68.07; H, 5.87; N, 5.26. FT-IR (in KBr): 3311, 2994, 2938, 2835, 1709, 1580, 1501, 1470, 1410, 1360, 1234, 1124, 1078, 1005, 922, 806 and 722 cm^{-1}. ^{1}H NMR (400 MHz, $CDCl_3$): δ_{ppm}, 8.97 (s, 8H), 7.48 (s, 8H), 4.19(s, 12H), 3.98(s, 24H), -2.77(s, 2H). ^{13}C NMR (100 MHz, $CDCl_3$): δ_{ppm}, 151.4, 137.9, 137.5,

120.0, 112.8, 61.33 and 56.4. UV-visible (CH_2Cl_2): 422 nm (ε/M^{-1} cm^{-1}, 4.54 × 10^5), 463 nm (ε/M^{-1} cm^{-1}, 1.16 × 10^4), 517 nm (ε/M^{-1} cm^{-1}, 2.09 × 10^4), 553 nm (ε/M^{-1} cm^{-1}, 8.25 × 10^3), 592 nm (ε/M^{-1} cm^{-1}, 6.13 × 10^3), 648 nm (ε/M^{-1} cm^{-1}, 4.75 × 10^3). ESI-mass (m/z): calculated, 975.381; found, 975.383 ($[M+H]^+$ peak).

[Mn(TTMPP^{2-})Cl], 1a:

To a 100 mL round bottom flask equipped with a magnetic stir bar, H_2TTMPP (975 mg, 1 mmol), $Mn(OAc)_2.4H_2O$ (2.45 g, 10 mmol) and KCl (745 mg, 10 mmol) was added followed by 50 mL 1:1 mixture of chloroform-acetic acid. The resulting mixture was refluxed for 12 h. After brought to room temperature, the reaction mixture was washed with water (3 × 100 mL) and extracted using chloroform (3 × 30 mL). The crude thus obtained was subjected to silica-column and complex **1a** was isolated as green solid. Yield ~ 90% (957 mg). Elemental analyses for $C_{56}H_{52}ClMnN_4O_{12}$ Calculated (%): C, 63.25; H, 4.93; N, 5.27. found (%): C, 62.59; H, 5.23; N, 4.95. FT-IR (in KBr): 1580, 1496, 1462, 1409, 1354, 1235, 1124, 1009, 947, 804 and 722 cm^{-1}. UV-visible (CH_2Cl_2): 482 nm (ε/M^{-1} cm^{-1}, 9.34 × 10^4), 529 nm (ε/M^{-1} cm^{-1}, 5.47 × 10^3), 583 nm (ε/M^{-1} cm^{-1}, 8.28 × 10^3), 619 nm (ε/M^{-1} cm^{-1}, 8.65 × 10^3). ESI-mass (m/z): calculated, 1027.296; found, 1027.296 ($[Mn(TTMPP^{2-})]^+$ ion peak). Crystal data: complex **1a**, CCDC No. 2349504. $C_{56}H_{52}N_4O_{12}Cl_2Mn$, M = 1098.86, Triclinic (P -1), a = 8.0273(4) Å, b = 12.4667(6) Å, c = 14.3129(7) Å, α = 86.5190(10)°, β = 75.1190(10)°, γ = 88.2800(10)°, V = 1381.60(12) $Å^3$, Z = 1, D_c = 1.321 g cm^{-3}, μ = 0.400 mm^{-1}, T = 298(2) K, 4862 reflections, 4109 independent, $R(F)$ = 0.0615 [$I > 2\delta(I)$], R(int) = 0.0741, $wR(F2)$ = 0.1998 (all data), GOF = 1.053.

[Mn(TTMPP^{2-})(NO)], 1:

Complex **1a** (41 mg, 0.04 mmol) was taken in a 25 ml Schlenk flask and degassed with consecutive vacuum/Argon cycles. Dry and distilled THF (2 mL) was added to it and the green-colored solution was cooled to -40 °C. To this solution, freshly prepared methanolic solution of hydroxylamine (5 mole equivalent) was added. The color of the solution changes from green to dark red. Precooled dry and degassed methanol (5 mL) is added to this red solution and kept at -40 °C for 24 hrs. Reddish-purple colored precipitate of complex **1** was obtained with ~75% yield (31.7 mg). Elemental analyses for $C_{56}H_{52}MnN_5O_{13}$ Calculated (%): C, 63.57; H, 4.95; N, 6.62. found (%): C, 62.85; H, 5.28; N, 5.98 FT-IR (in KBr): 2936, 2833, 1747, 1580, 1499, 1463, 1409, 1355, 1236, 1126, 1004, 946, 802 and 723 cm^{-1}. ^1H NMR (400 MHz, $CDCl_3$): δ_{ppm}, 9.44 (s, 8H), 7.49 (s, 8H), 4.19(s, 12H), 3.97(s, 24H). UV-visible (CH_2Cl_2): 416 nm (ε/M^{-1} cm^{-1}, 1.20×10^5), 534 nm (ε/M^{-1} cm^{-1}, 1.26×10^4), 561 nm (ε/M^{-1} cm^{-1}, 6.90×10^3). ESI-mass (m/z): calculated, 1058.302; found, 1058.440 ($[M+H]^+$ peak).

[Mn^{III}(TTMPP^{2-})(OH)], 2a:

Complex **1** (53 mg, 0.05 mmol) was taken in a 15 mL Schlenk tube and degassed properly with consecutive Argon/vacuum purge. Addition of dry and degassed dichloromethane to the Schlenk tube results in a red color solution. Upon keeping the solution under visible light, the red color solution turns into green. The solvent was removed under vacuum. Green crude product obtained with ~ 90% yield (47 mg). Crystals were obtained by slow evaporation of dichloromethane solution of the complex. Elemental analyses for $C_{56}H_{53}MnN_4O_{13}$ Calculated (%): C, 64.37; H, 5.11; N, 5.36. found (%): C, 63.89; H, 4.82; N, 5.16. FT-IR (in KBr): 3435, 2931, 1580, 1497, 1464, 1411, 1355, 1206, 1163, 1124, 1006, 947, 862 and 722 cm^{-1}. UV-visible (CH_2Cl_2): 484 nm (ε/M^{-1} cm^{-1}, 7.44×10^4), 520 nm (ε/M^{-1} cm^{-1}, 7.02×10^3), 577 nm (ε/M^{-1} cm^{-1}, 1.08×10^4), 611 nm (ε/M^{-1} cm^{-1}, 8.82×10^3), 783 nm (ε/M^{-1} cm^{-1}, 1.33×10^3).

ESI-mass (m/z): calculated, 1027.296; found, 1027.297 ($[Mn(TTMPP^{2-})]^+$ ion peak, after removal of OH^- group). Crystal data: complex **2a**, CCDC No. 2349505. $C_{56}H_{54}N_4O_{14}Mn$, M = 1061.97, Triclinic (P -1), a = 7.981(3) Å, b = 12.383(5) Å, c = 14.282(6) Å, α = 85.706(12)°, β = 76.649(12)°, γ = 87.299(13)°, V = 1368.9(9) Å^3, Z = 1, D_c = 1.288 g cm^{-3}, μ = 0.309 mm^{-1}, T = 298.0 K, 6126 reflections, 4129 independent, $R(F)$ = 0.0728 [$I > 2\delta(I)$], R(int) = 0.1118, $wR(F2)$ = 0.1998 (all data), GOF = 1.059.

$[Mn^{III}(TTMPP^{2-})(CH_3OH)_2](BPh_4)$, 2b:

Complex **1** (53 mg, 0.05 mmol) was taken in a 15 mL Schlenk tube and degassed properly with consecutive Argon/vaccum purge. Addition of dry and degassed dichloromethane to the Schlenk tube results in a red color solution. Upon keeping the complex solution under visible light, the red color solution turns into green. To this green solution, dry and degassed methanolic solution of $NaBPh_4$ (1.5 equivalent) was added. After 1 h of the addition, the solvent was removed under vaccum. Green crude obtained with ~86% yield (58 mg). Crystals were obtained by layering methanol over Chloroform solution of the complex. Elemental analyses for $C_{82}H_{80}BMnN_4O_{14}$ Calculated (%): C, 69.79; H, 5.71; N, 3.97. found (%): C, 70.12; H, 5.48; N, 4.23. FT-IR (in KBr): 2933, 1579, 1492, 1460, 1408, 1353, 1310, 1235, 1163, 1124, 1008, 946, 805, 724 and 704 cm^{-1}. UV-visible (CH_2Cl_2): 482 nm (ε/M^{-1} cm^{-1}, 4.53 × 10^4), 527 nm (ε/M^{-1} cm^{-1}, 4.47 × 10^3), 576 nm (ε/M^{-1} cm^{-1}, 1.51 × 10^4), 614 nm (ε/M^{-1} cm^{-1}, 6.31 × 10^3), 710 nm (ε/M^{-1} cm^{-1}, 6.95 × 10^2). ESI-mass (m/z): calculated, 1027.296; found, 1027.296 ($[Mn(TTMPP^{2-})]^+$ ion peak). Crystal data: complex **2b**, CCDC No. 2349506 $C_{83}H_{81}BN_4O14Cl_3Mn$, M = 1530.62, Monoclinic (P 21/c), a = 15.425(5) Å, b = 22.911(7) Å, c = 25.451(8) Å, α = 90°, β = 105.144(9)°, γ = 90°, V = 8682(5) Å^3, Z = 4, D_c = 1.171 g cm^{-3},

μ = 0.304 mm^{-1}, *T* = 297.00 K, 19273 reflections, 12494 independent, *R*(*F*) = 0.0960 [*I* > 2δ(*I*)], *R*(int) = 0.1420, *wR*(*F2*) = 0.2688 (all data), GOF = 1.073.

[Mn^{III}($TTMPP^{2-}$)Cl], 1a isolated from the reaction mixture of complex 1 and [Fe^{III}(TPP)Cl]:

To a 25 mL Schlenk flask equipped with a magnetic stir-bar, complex **1** (53 mg, 0.05 mmol) and [Fe^{III}(TPP)Cl] (42 mg, 0.06 mmol) was added and degassed by consecutive Argon/vaccum purge. Dry and degassed dichloromethane was added to it and the reaction mixture was allowed to stir under visible light at -40 °C for 1 h. After bringing the reaction mixture to room temperature, the solvent was removed under vacuo. The green crude obtained was subjected to column chromatography. Complex **1a** was obtained with ~81% yield (43 mg). Elemental analyses for $C_{56}H_{52}ClMnN_4O_{12}$ Calculated (%): C, 63.25; H, 4.93; N, 5.27. found (%): C, 62.89; H, 5.13; N, 5.01. FT-IR (in KBr): 1580, 1496, 1462, 1409, 1354, 1235, 1124, 1009, 947, 804 and 722 cm^{-1}. UV-visible (CH_2Cl_2): 482 nm (ε/M^{-1} cm^{-1}, 9.34 × 10^4), 529 nm (ε/M^{-1} cm^{-1}, 5.47 × 10^3), 583 nm (ε/M^{-1} cm^{-1}, 8.28 × 10^3), 619 nm (ε/M^{-1} cm^{-1}, 8.65 × 10^3). ESI-mass (m/z): calculated, 1027.296; found, 1027.296 ([Mn($TTMPP^{2-}$)]$^+$ ion peak).

[Mn^{III}($TTMPP^{2-}$)(DTC)], 3 isolated from the reaction mixture of complex 1 and [$Fe^{III}(DTC)_3$]:

To a 25 mL Schlenk flask equipped with a magnetic stir-bar, complex **1** (53 mg, 0.05 mmol) and [$Fe^{III}(DTC)_3$] (30 mg, 0.06 mmol) was added and degassed by consecutive Argon/vaccum purge. Dry and degassed dichloromethane was added to it and the reaction mixture was allowed to stir in the presence of visible light at -40 °C for 1 h. After bringing the reaction mixture to room temperature, the solvent was removed under vacuo. Complex **3** was obtained from the reaction mixture by subjecting it to column chromatography with ~86% yield (52 mg). Elemental analyses for $C_{61}H_{62}MnN_5O_{12}S_2$ Calculated (%): C, 62.29; H, 5.31; N, 5.95. found

(%): C, 61.78; H, 5.08; N, 5.57. FT-IR (in KBr): 2925, 1629, 1580, 1498, 1464, 1411, 1355, 1236, 1164, 1124, 1005, 947, 804 and 722 cm^{-1}. UV-visible (CH_2Cl_2): 483 nm (ε/M^{-1} cm^{-1}, 1.21×10^5), 521 nm (ε/M^{-1} cm^{-1}, 1.28×10^4), 576 nm (ε/M^{-1} cm^{-1}, 1.82×10^4), 611 nm (ε/M^{-1} cm^{-1}, 1.50×10^4), 783 nm (ε/M^{-1} cm^{-1}, 2.77×10^3). ESI-mass (m/z): calculated, 1215.346; found, 1215.746 ($[M+K]^+$ ion peak).

$[Fe^{III}(TPP)(Cl)]$ ($TPPH_2$ = 5,10,15,20-Tetraphenylporphyrin):

To a 50 mL round bottom flask, $FeCl_3 \cdot 6H_2O$ (5 mmol, 1.35 g) and H_2TPP (0.5 mmol, 0.31 g) were added and dissolved in 20 mL dimethylformamide. The solution was refluxed while stirring for 4 h. After cooling to room temperature, water was added to precipitate out the crude solid and filtered. Purification using column chromatography yielded purple solid of $[Fe^{III}(TPP)(Cl)]$. Yield *ca.* 50% (0.20 g). Elemental analyses for $C_{44}H_{28}N_4ClFe$ Calcd (%): C, 75.07; H, 4.01; N, 7.96. found (%): C, 74.89; H, 4.19; N, 7.52. UV–visible (CH_2Cl_2): 416 nm (ε/M^{-1} cm^{-1}, 1.32×10^5), 509 nm (ε/M^{-1} cm^{-1}, 1.30×10^4), 570 nm (ε/M^{-1} cm^{-1}, 5.26×10^3), and 690 nm (ε/M^{-1} cm^{-1}, 1.91×10^3). FT-IR (in KBr): 1596, 1486, 1442, 1337, 1202, 1175, 1070, 1000, 998, 807, 752, and 704 cm^{-1}. ESI-mass (m/z): calculated, 668.166; found, 668.166 ($[Fe^{III}(TPP)]^+$ ion peak).

$[Fe^{III}(DTC)_3]$ (DTC^- = Diethyldithiocarbamate anion): $FeCl_3 \cdot 6H_2O$ (1 mmol, 0.27 g) was taken in a 50 mL round bottom flask and dissolved in 10 mL ethanol by stirring. An ethanolic solution of sodium diethyldithiocarbamate trihydrate (3 mmol, 0.68 g in 20 mL) was added slowly to this stirred solution. The addition results in to the immediate precipitation. The stirring was continued for 1 h and the precipitate was filtered off. The product was recrystallized from hot toluene. Dark brown crystalline product obtained. $[Fe^{III}(DTC)_3]$. Yield *ca.* 82% (0.45 g). Elemental analyses for $C_{10}H_{20}N_3OS_4Fe$ Calcd (%): C, 31.41; H, 5.27; N, 10.99. found (%): C, 31.68; H, 5.02; N, 10.68. UV–visible (in CH_2Cl_2): 347 nm (ε/M^{-1} cm^{-1},

1.41 × 10^4), 385 nm (ε/M^{-1} cm^{-1}, 1.15 × 10^4), 510 nm (ε/M^{-1} cm^{-1}, 3.52 × 10^3), and 592 nm (ε/M^{-1} cm^{-1}, 2.85 × 10^3). FT-IR (in KBr): 1494, 1456, 1450, 1434, 1376, 1355, 1296, 1270, 1205, 1142, 1134, 1077, 991, 910, 845, and 784 cm^{-1}. ESI-mass (m/z): calcd, 500.011; found, 500.012 (molecular ion peak).

Reaction of complex 1 with [Fe^{III}(TPP)Cl]: Complex **1** (21 mg, 0.02 mmol) and [Fe^{III}(TPP)Cl] (14 mg, 0.02 mmol) were taken in a Schlenk flask and degassed it by applying consecutive vaccum/Ar purge. The reaction vessel was cooled to -40 °C and precooled dichloromethane (dry and degassed, 2 mL) was added to it and stirred under visible light. After the reaction mixture brought to room temperature, the reaction was monitored in FT-IR and EPR spectroscopic techniques.

Reaction of complex 1 with [$Fe^{III}(DTC)_3$]: Complex **1** (21 mg, 0.02 mmol) and [$Fe^{III}(DTC)_3$] (10.02 mg, 0.02 mmol) were taken in a Schlenk flask and degassed it by applying consecutive vaccum/Ar purge. The reaction vessel was cooled to -40 °C and precooled dichloromethane (dry and degassed, 2 mL) was added to it and stirred under visible light. After the reaction mixture brought to room temperature, the reaction was monitored in FT-IR and EPR spectroscopic techniques.

Reaction of complex 1 with Triphenylphosphine in presence of $HBF_4.Et_2O$: A mixture of complex **1** (10. mg, 0.01 mmol) and PPh_3 (0.08 g, 0.03 mmol) was dissolved in 0.4 mL of dry and degassed dichloromethane under argon atmosphere. To this reaction mixture, $HBF_4.Et_2O$ (2 μL, 1.3 equivalent) was added and ^{31}P NMR was recorded in CD_3CN. ^{31}P-NMR (202 MHz, CD_3CN): $\delta_{ppm,}$ 26.75 ($Ph_3P{=}O$), 22.18 ($Ph_3P{=}NH$) and 44.26 (Metal-bound PPh_3).

Determination of the Yield of N_2O: N_2O for the calibration curve was produced using a previously reported procedure.[6] Different amount of N-hydroxybenzenesulfonamide was taken in five 15 mL Schlenk tube and degassed using vacuum/Ar purge. 0.1 M NaOH solution (10

mL) was added to each flask under the sealed condition. 1 mL of headspace gas from each reaction vessel was subjected to GC. By calculating the peak area at 2.79 min (corresponding to N_2O) for each set, a calibration curve of the concentration of N-hydroxybenzenesulfonamide was drawn.

Complex **1** (0.025 mmol, 0.026 g) in 15 mL of dry and degassed dichloromethane was taken in a 25 mL round-bottom flask and 50 μL of $HBF_4 \cdot Et_2O$ was added to it under argon atmosphere and stirred for ½ h in the presence of light. After the completion of the reaction, 1 mL of headspace gas was subjected to GC and amount of N_2O was measured from the calibration curve. Yield: *ca.* ~ 83%.

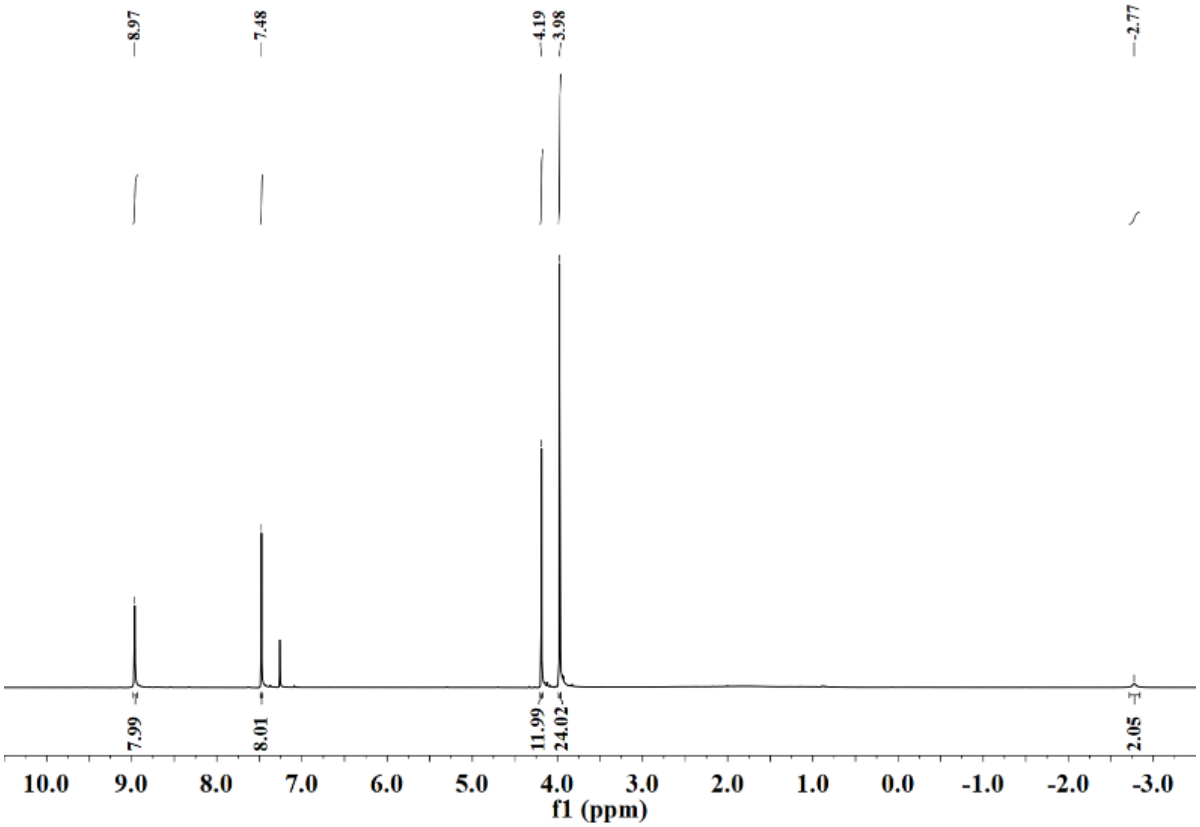

Figure S1. ^{1}H NMR spectrum of **H_2TTMPP** in $CDCl_3$.

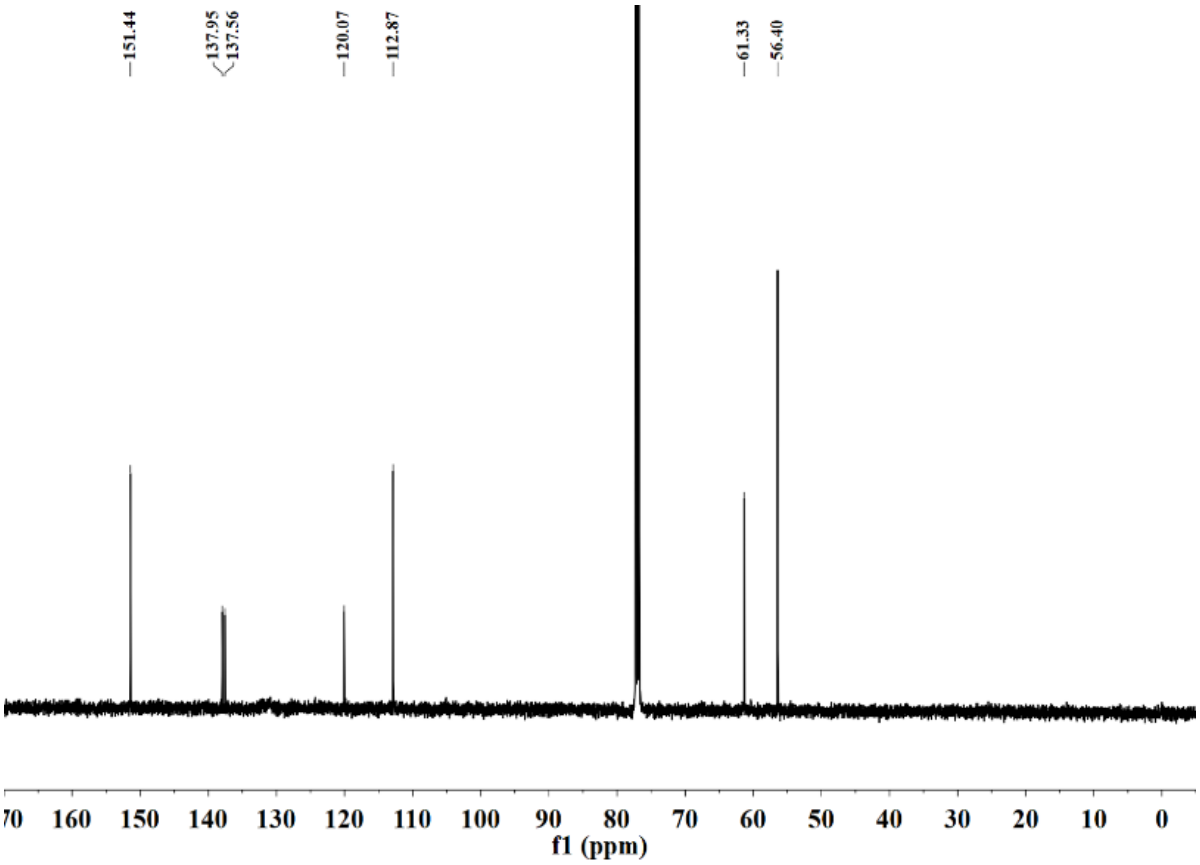

Figure S2. ^{13}C NMR spectrum of **H_2TTMPP** in $CDCl_3$.

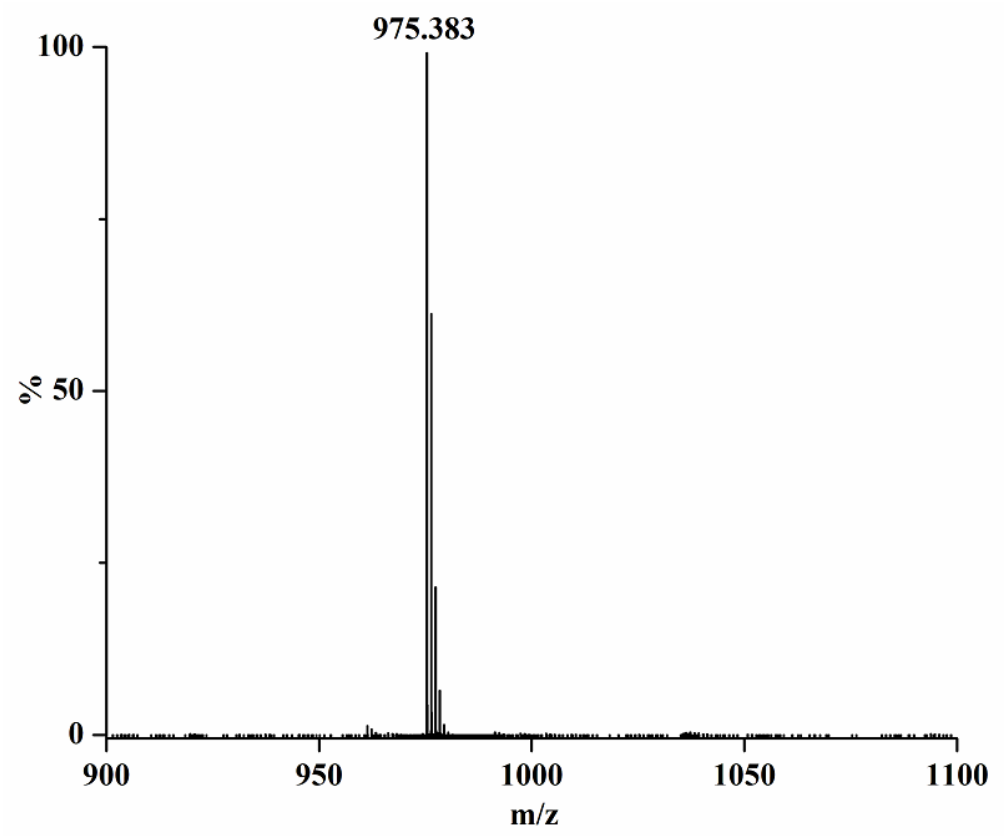

Figure S3. ESI-mass spectrogram of **H_2TTMPP** in methanol.

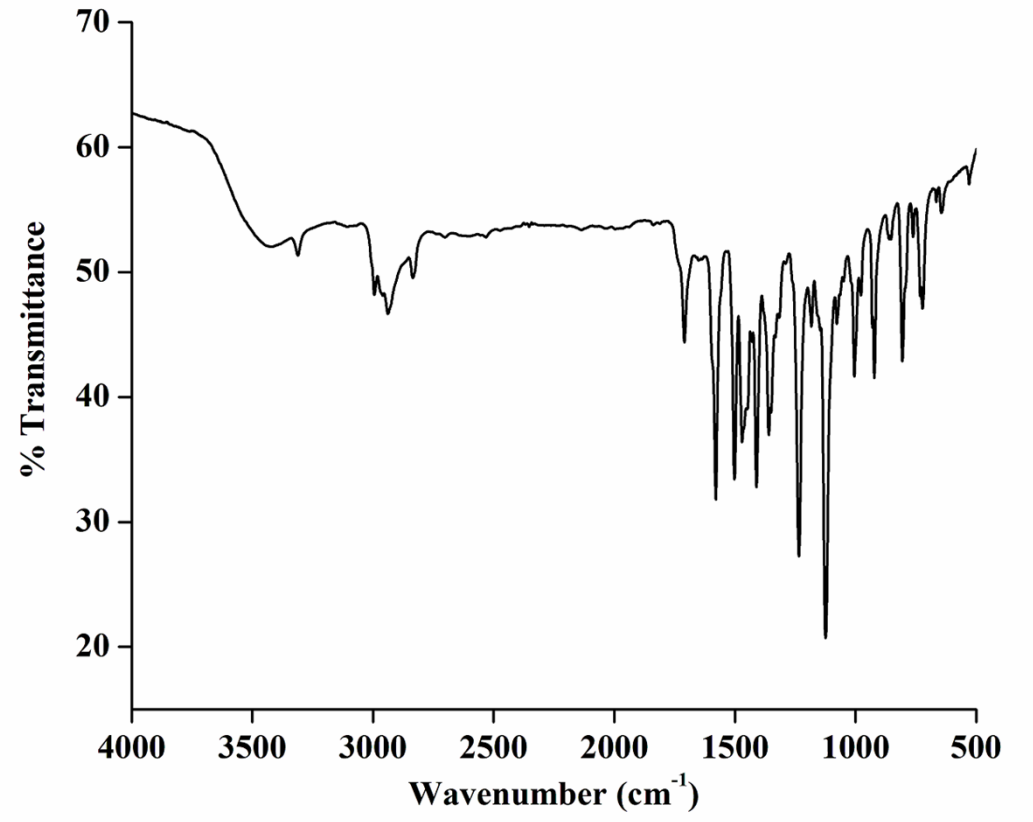

Figure S4. FT-IR spectrum of ligand **H_2TTMPP** in ATR probe.

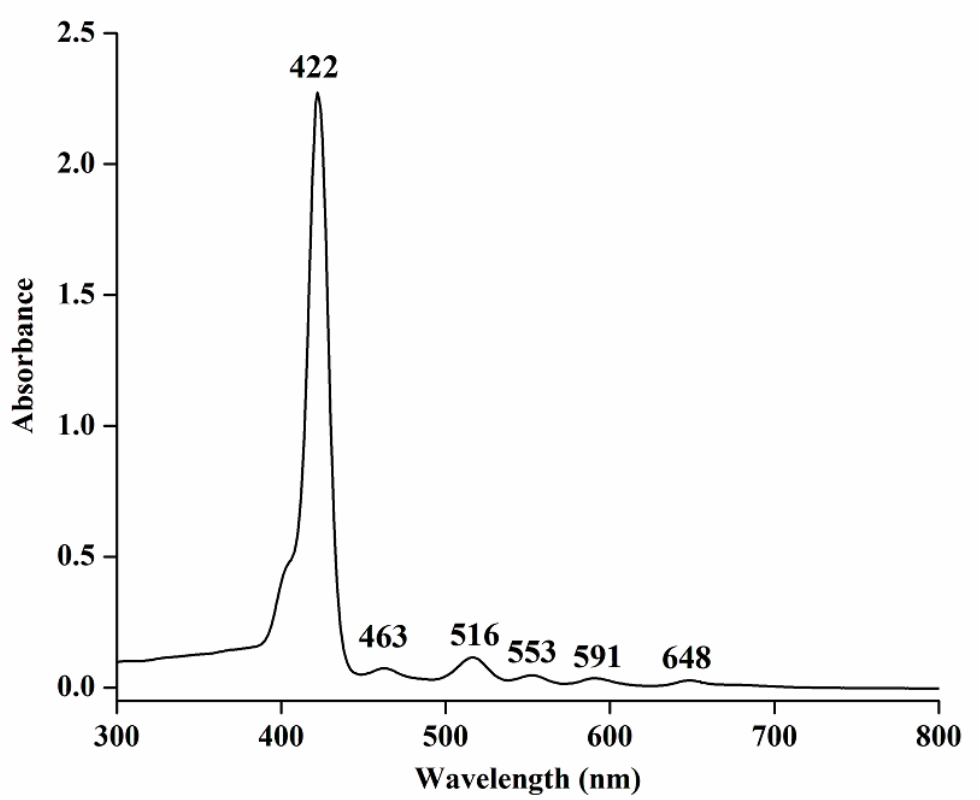

Figure S5. UV-visible spectrum of **H_2TTMPP** in dichloromethane.

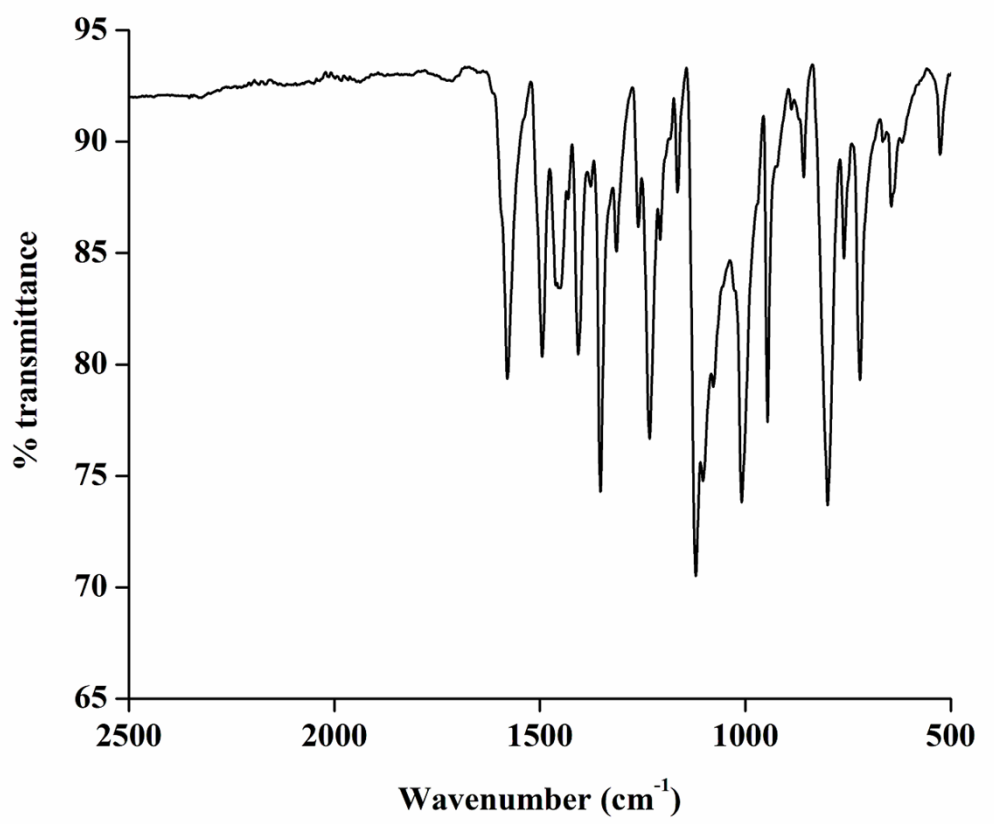

Figure S6. FT-IR spectrum of **[Mn(TTMPP^{2-})Cl]** in ATR probe.

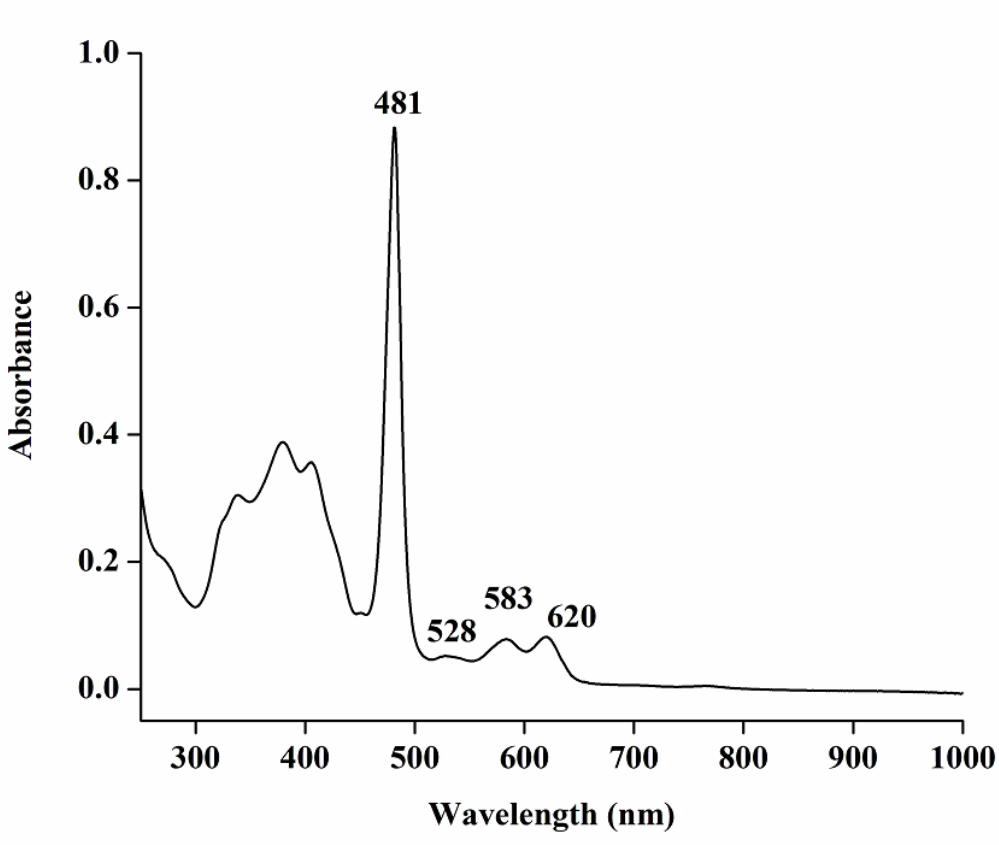

Figure S7. UV-visible spectrum of **[Mn(TTMPP^{2-})Cl]** in dichloromethane.

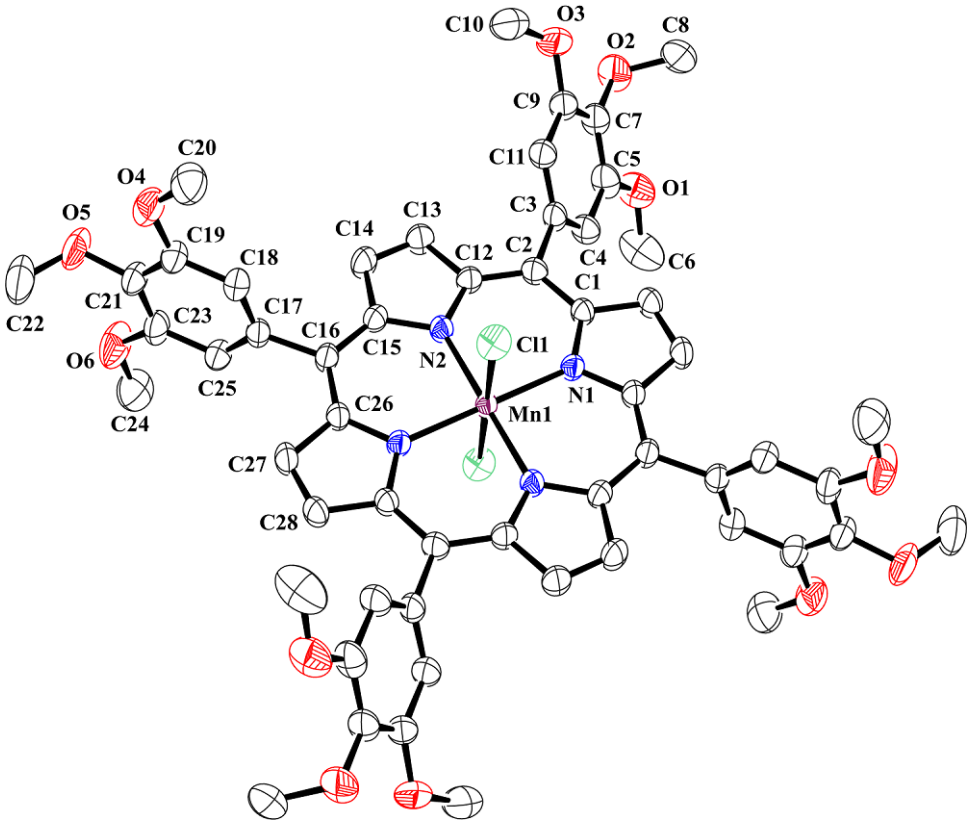

Figure S8. ORTEP of **[Mn(TTMPP^{2-})Cl]** (30% thermal ellipsoid plot. H-atoms are omitted for clarity).

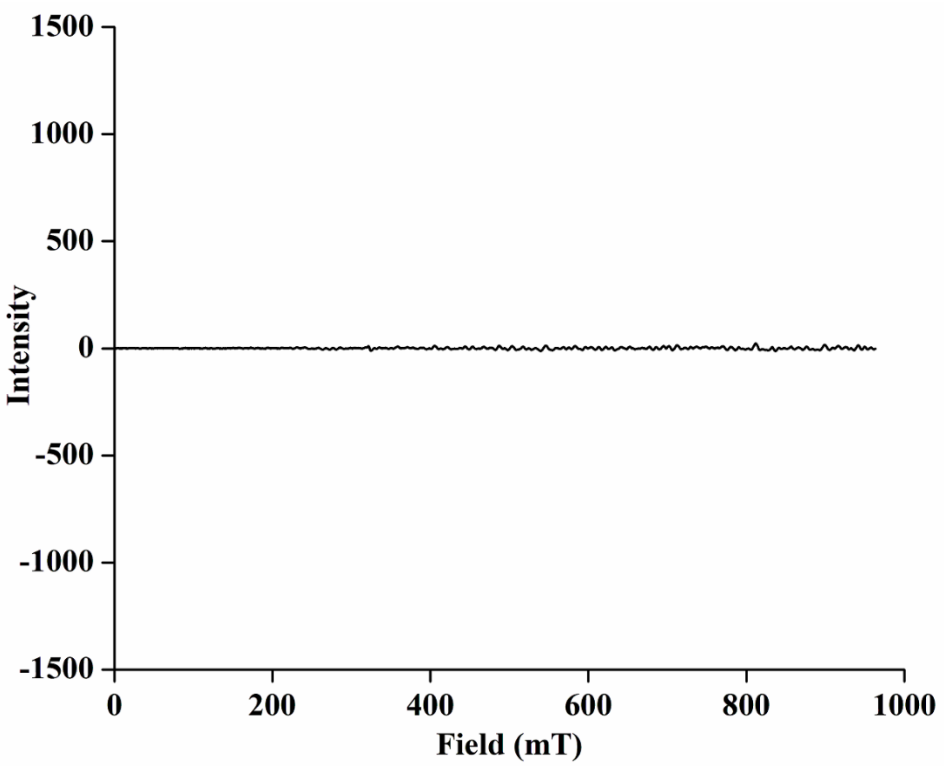

Figure S9. X-band EPR-spectrum of **[Mn(TTMPP^{2-})Cl]** in dichloromethane at 77 K.

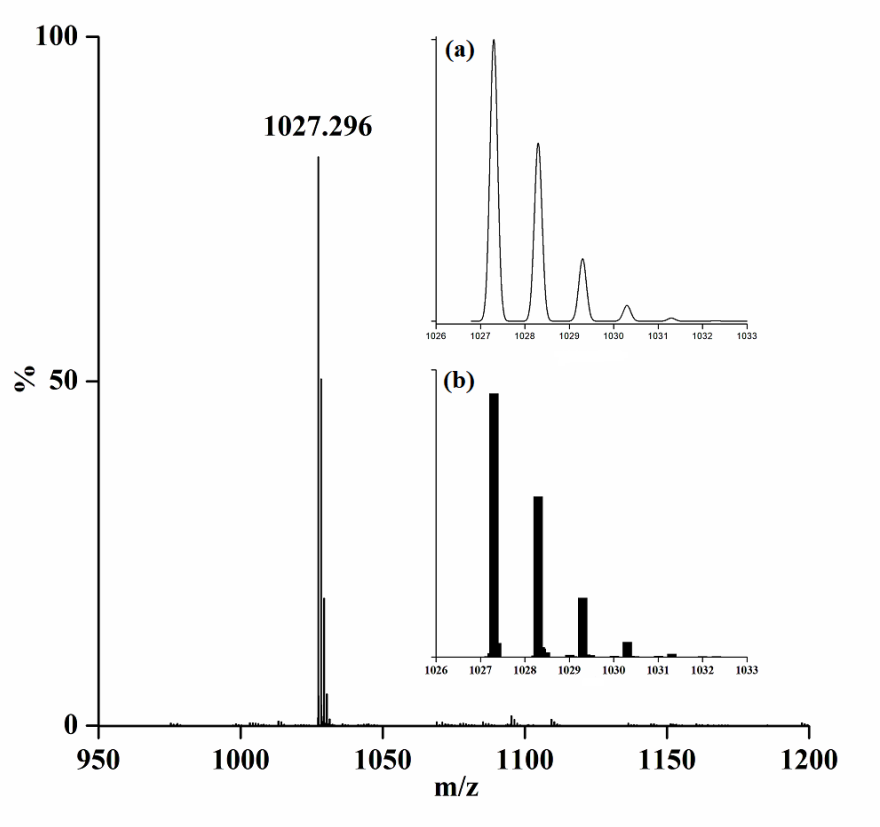

Figure S10. ESI-mass spectrogram of **[Mn(TTMPP^{2-})Cl]** in methanol. [Inset: (a) simulated and (b) experimental isotopic distribution pattern.]

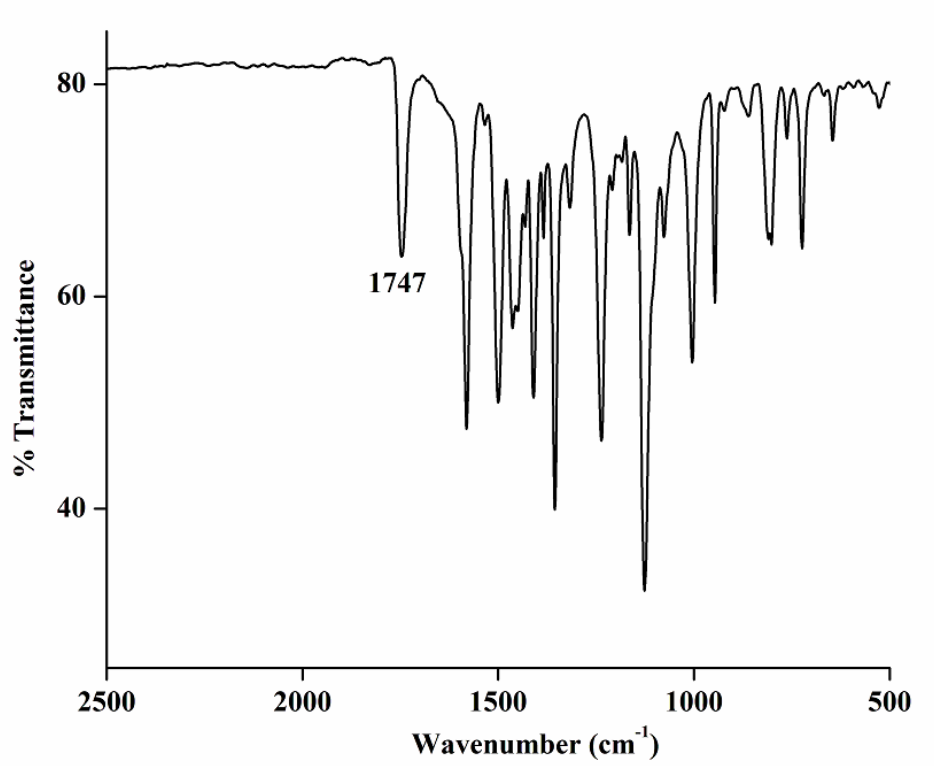

Figure S11. FT-IR spectrum of **[Mn(TTMPP^{2-})(NO)]** in ATR probe.

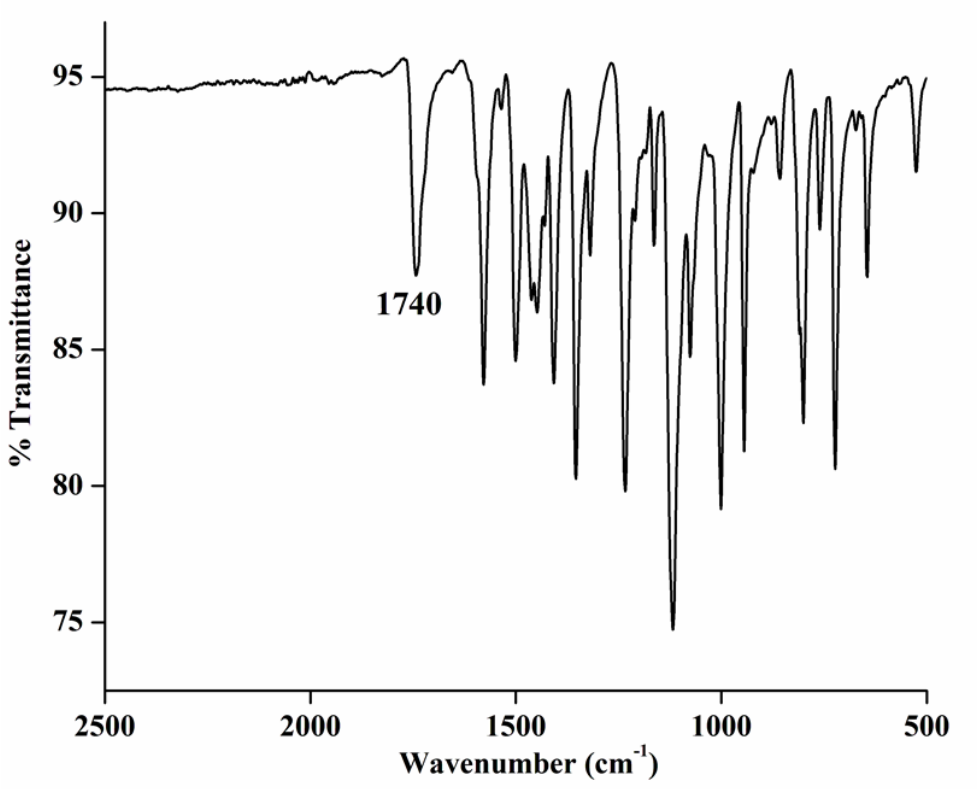

Figure S12. FTIR spectrum of **[Mn(TTMPP^{2-})(NO)]** in dichloromethane solution.

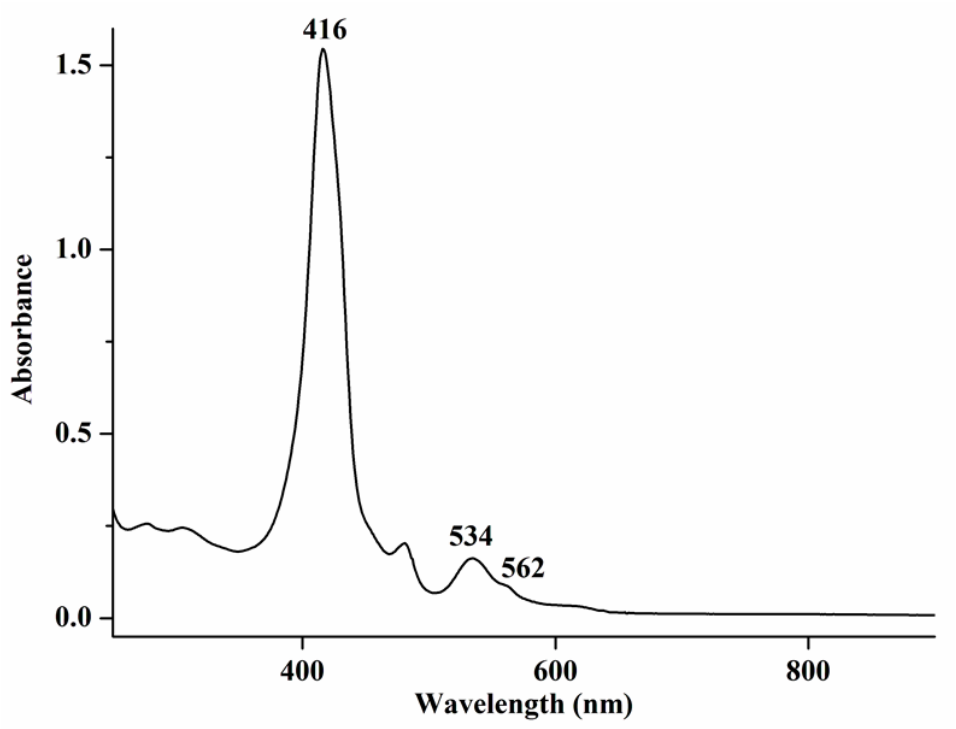

Figure S13. UV-visible spectrum of **[Mn(TTMPP^{2-})(NO)]** in dichloromethane at – 40 °C.

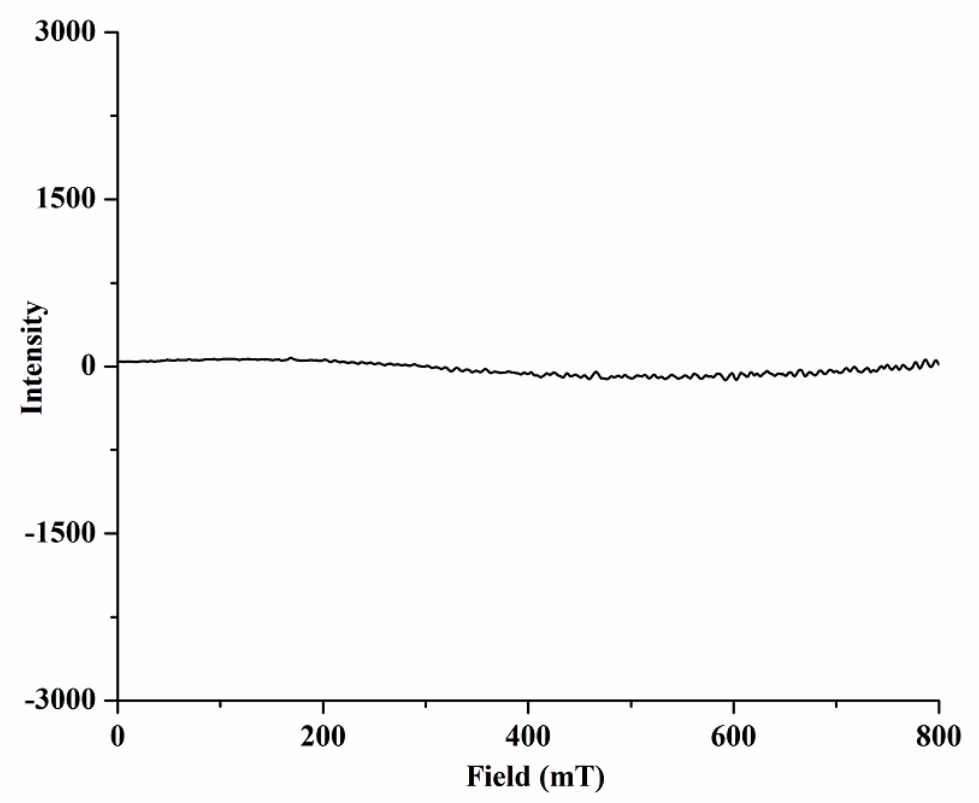

Figure S14. X-band EPR-spectrum of **[Mn(TTMPP^{2-})(NO)]** in dichloromethane at 77 K.

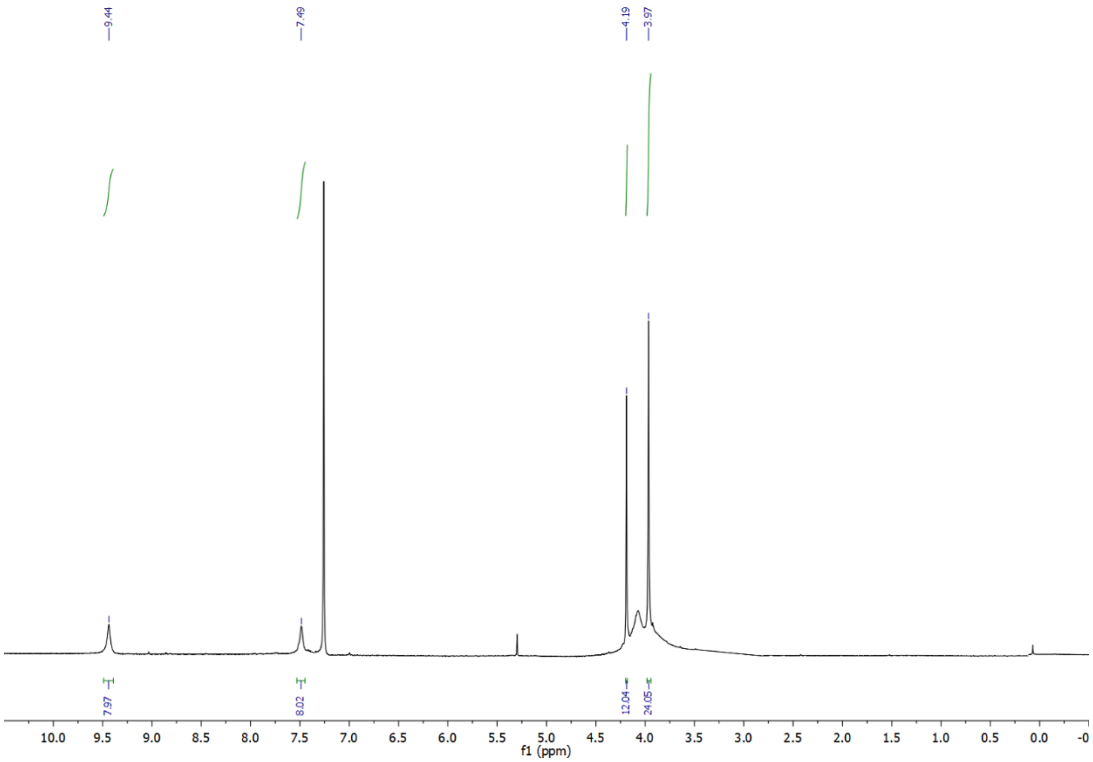

Figure S15. ^{1}H NMR spectrum of **[Mn(TTMPP^{2-})(NO)]** in $CDCl_3$.

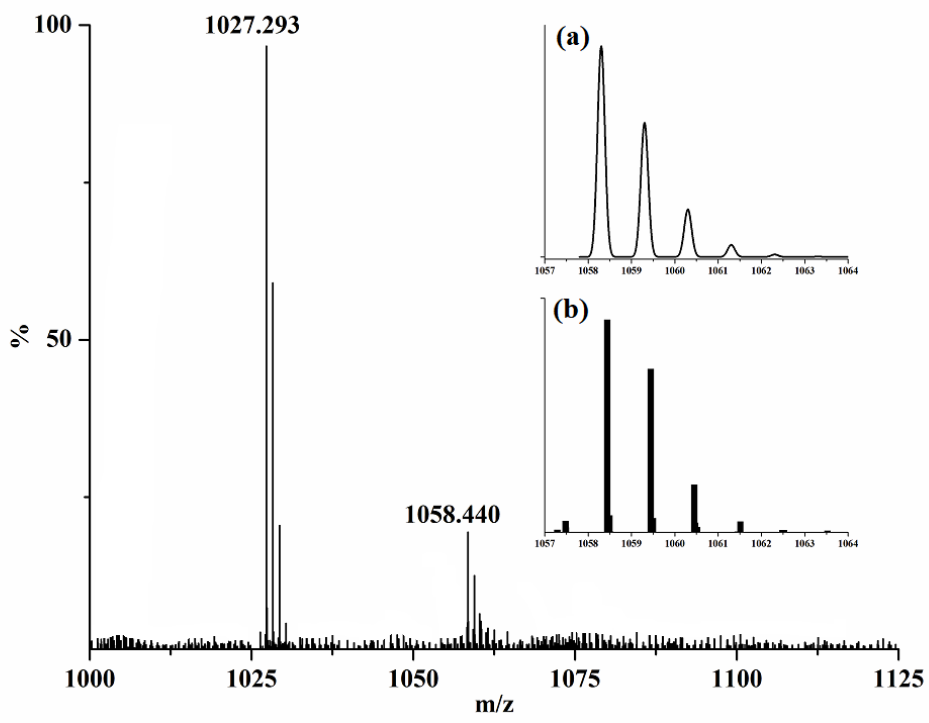

Figure S16. ESI-mass spectrogram of **[Mn(TTMPP^{2-})(NO)]** in methanol. [Inset: (a) simulated and (b) experimental isotopic distribution pattern.]

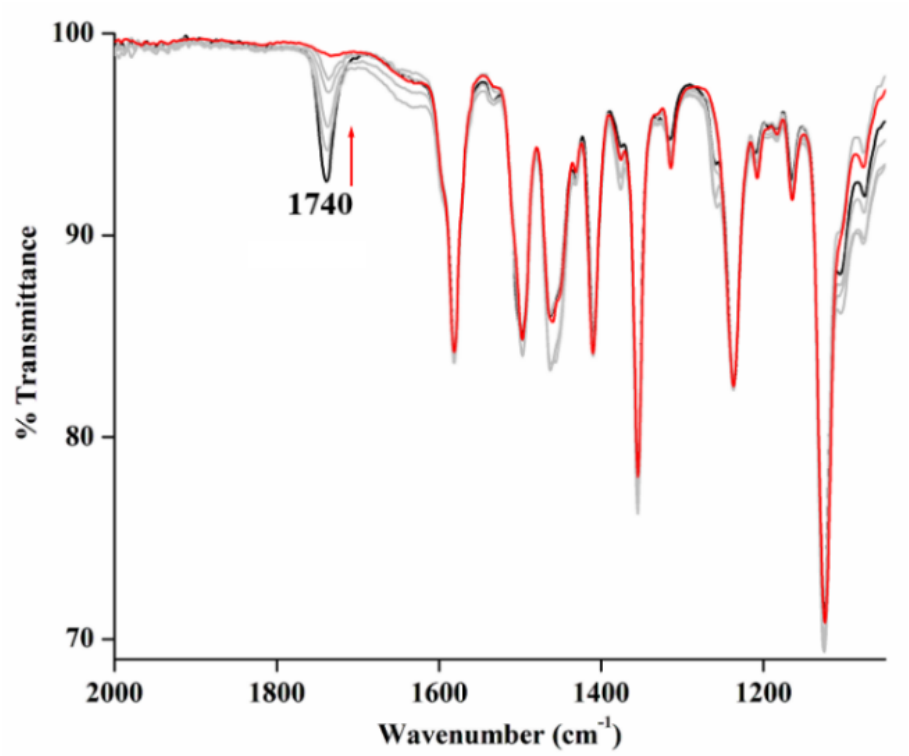

Figure S16b. FT-IR spectroscopic study of decomposition of complex **1** in dichloromethane solution in ATR probe [black (initial), red (final)].

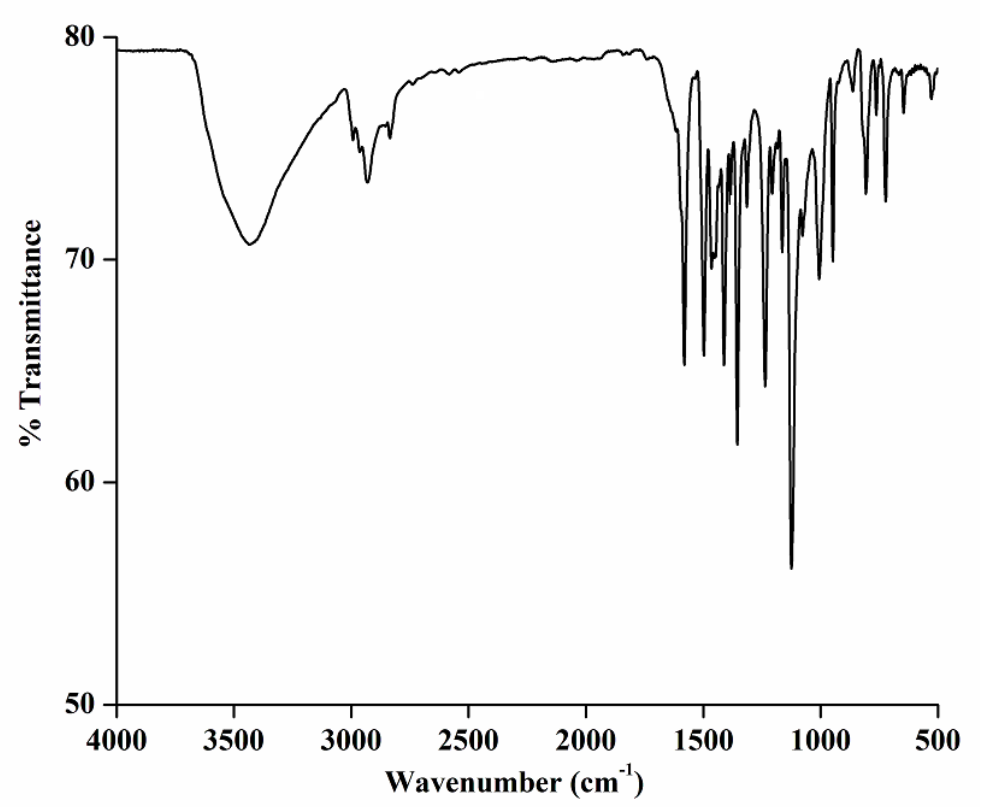

Figure S17. FT-IR spectrum of complex **[(TTMPP^{2-})Mn^{III}(OH)]** in ATR probe.

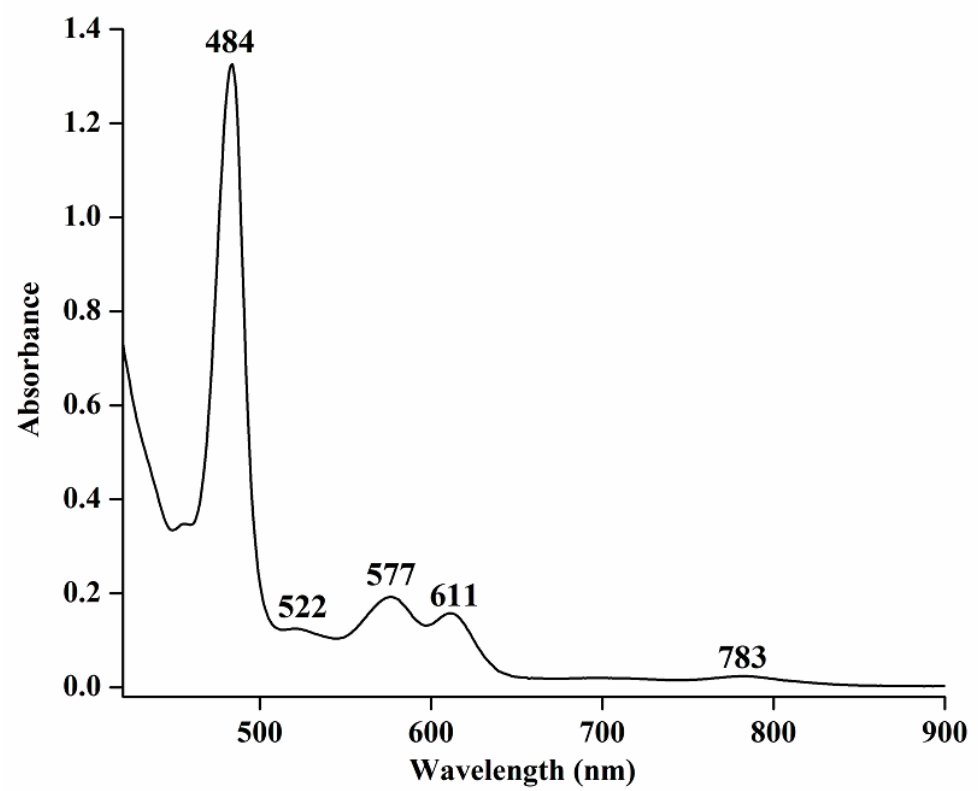

Figure S18. UV-visible spectrum of complex **[(TTMPP^{2-})Mn^{III}(OH)]** in dichloromethane.

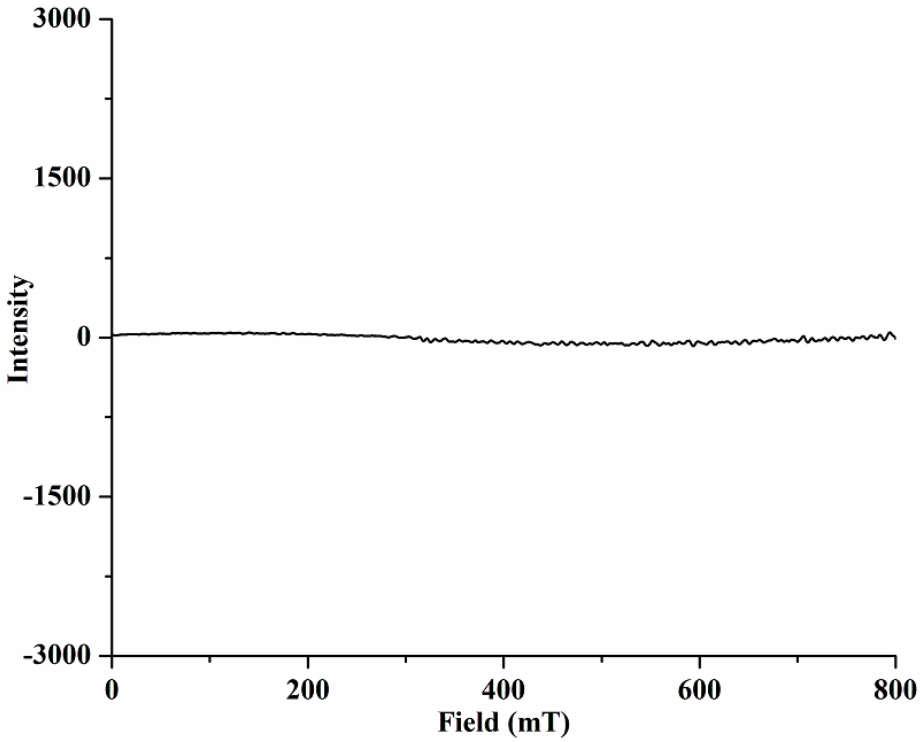

Figure S19. X-band EPR-spectrum of complex **[(TTMPP^{2-})Mn^{III}(OH)]** in dichloromethane at 77 K.

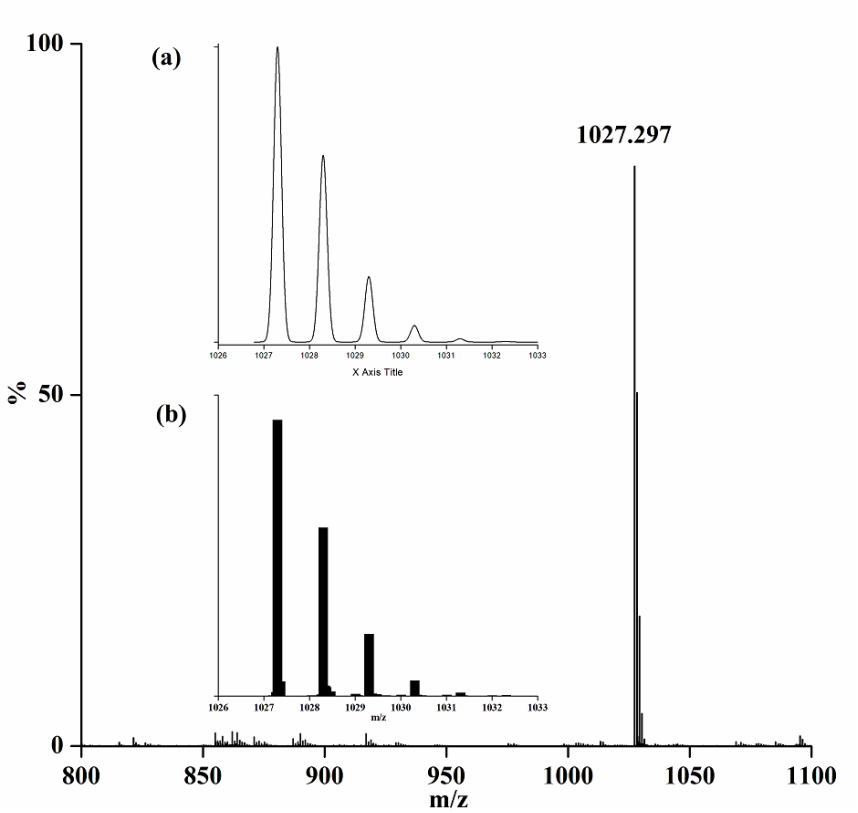

Figure S20a. ESI-mass spectrogram of **[(TTMPP^{2-})Mn^{III}(OH)]** in methanol. [Inset: (a) simulated and (b) experimental isotopic distribution pattern.]

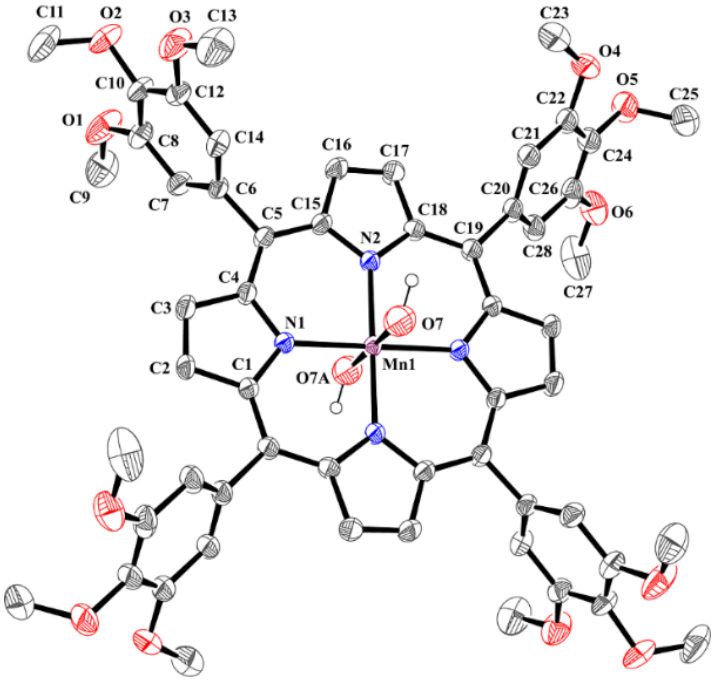

Figure S20b. ORTEP diagram of complex **2a** (40% thermal ellipsoid plot, H-atoms (except OH hydrogen) are omitted for clarity).

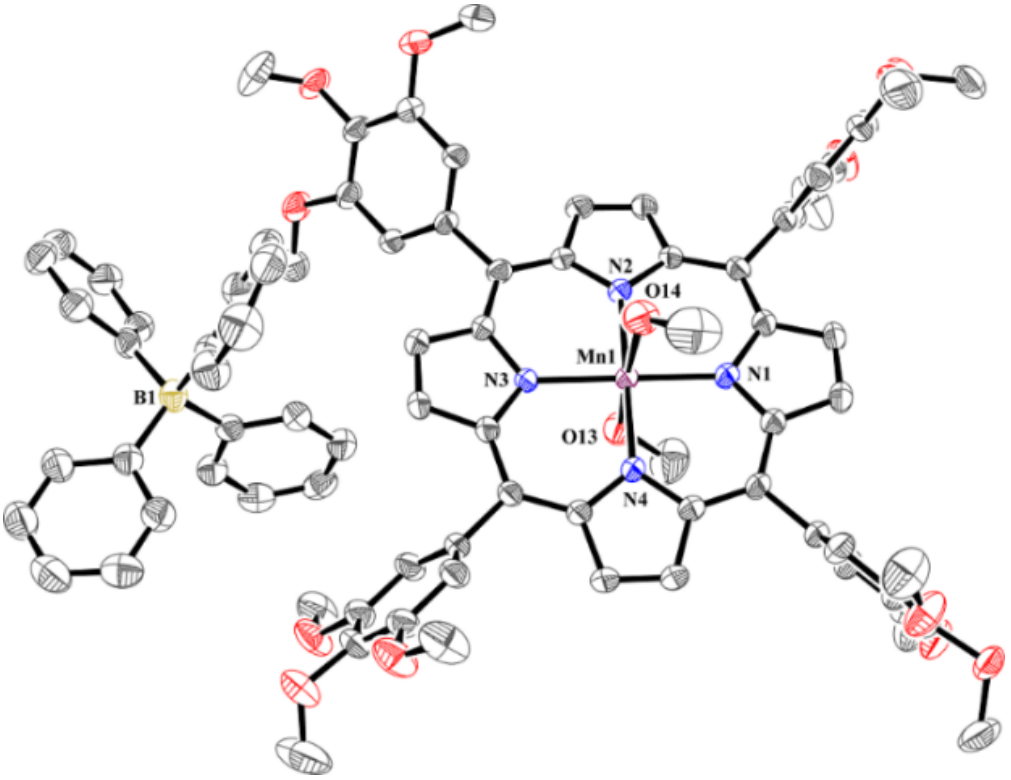

Figure S21. ORTEP diagram of complex **2b** (40% thermal ellipsoid plot, solvent ($CHCl_3$) and H-atoms are omitted for clarity)

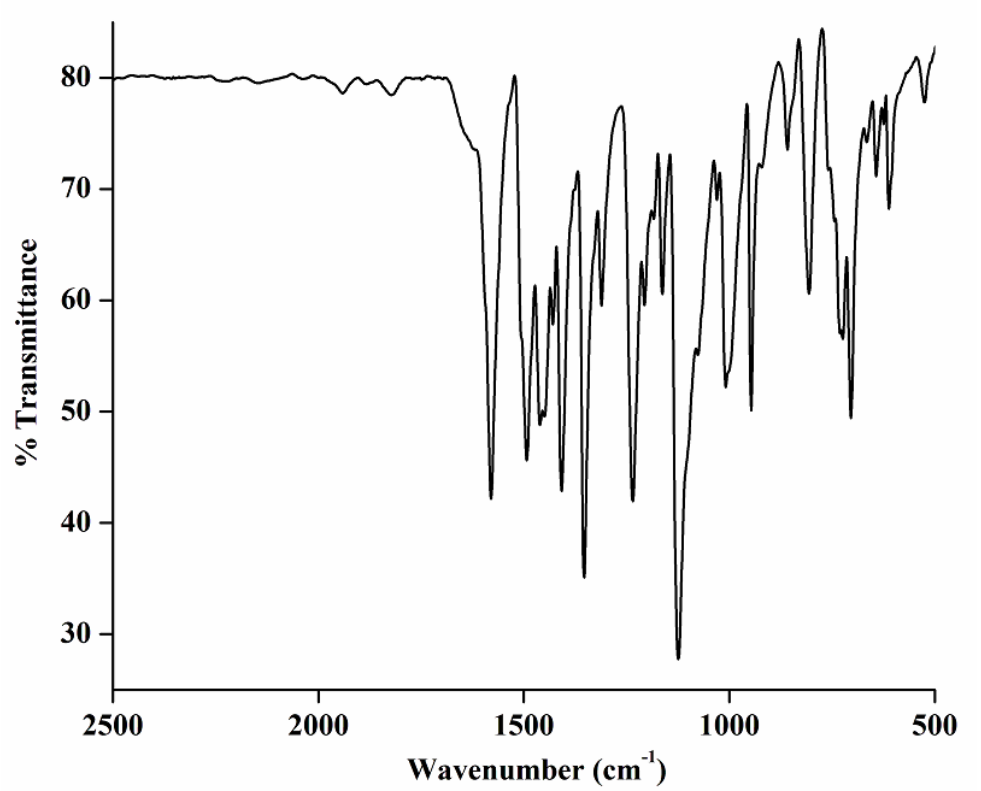

Figure S22. FT-IR spectrum of complex **[(TTMPP^{2-})Mn^{III}](BPh$_4$)** in ATR probe.

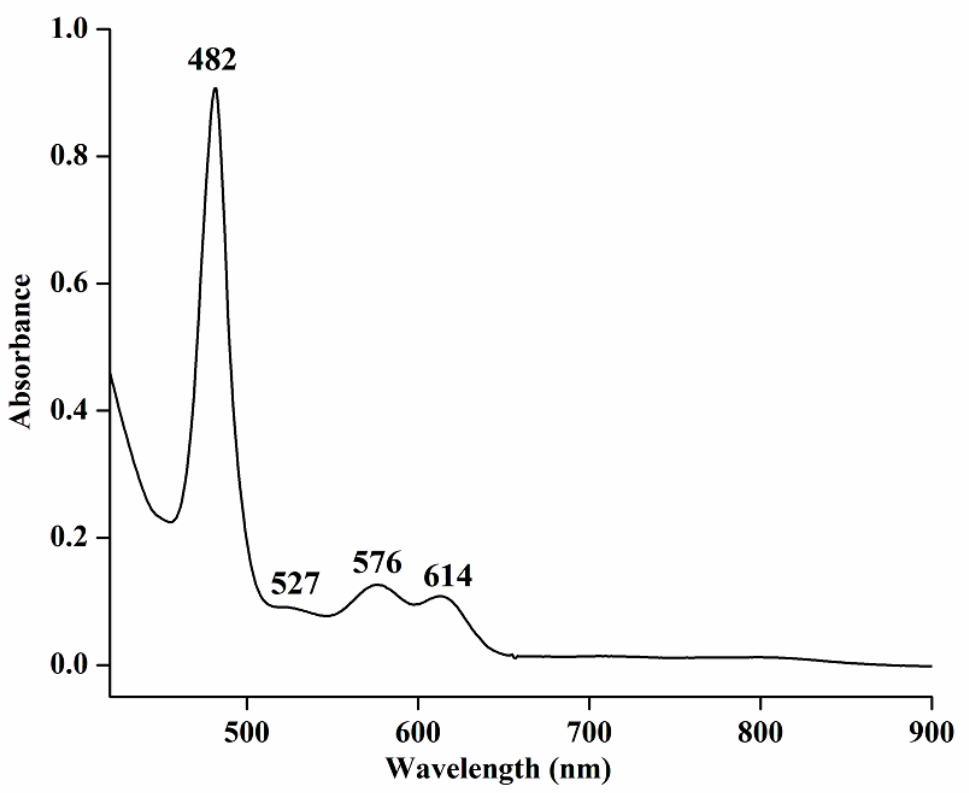

Figure S23. UV-visible spectrum of complex **[(TTMPP^{2-})Mn^{III}](BPh$_4$)** in dichloromethane.

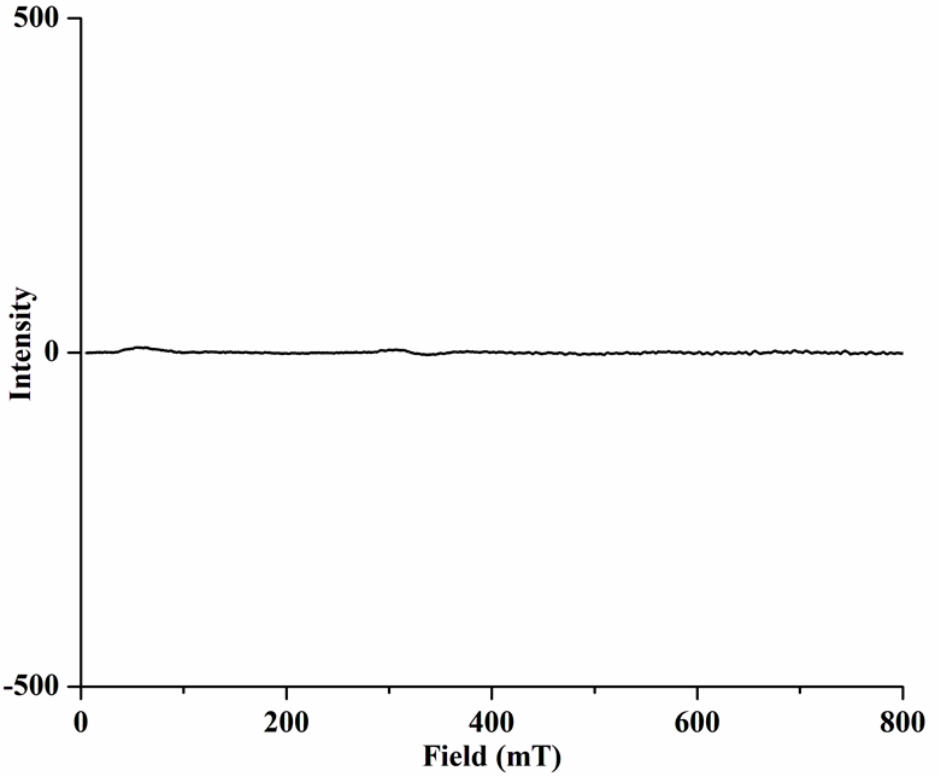

Figure S24. X-band EPR-spectrum of complex **[(TTMPP^{2-})Mn^{III}](BPh$_4$)** in dichloromethane at 77 K.

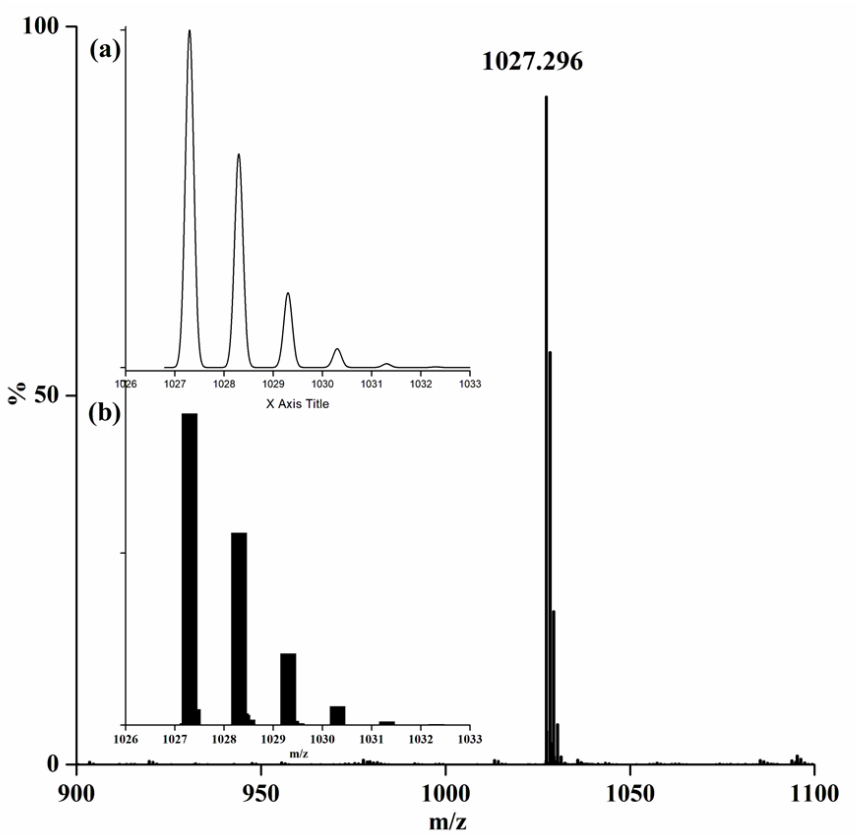

Figure S25. ESI-mass spectrogram of **[(TTMPP^{2-})Mn^{III}](BPh$_4$)** in methanol. [Inset: (a) simulated and (b) experimental isotopic distribution pattern.]

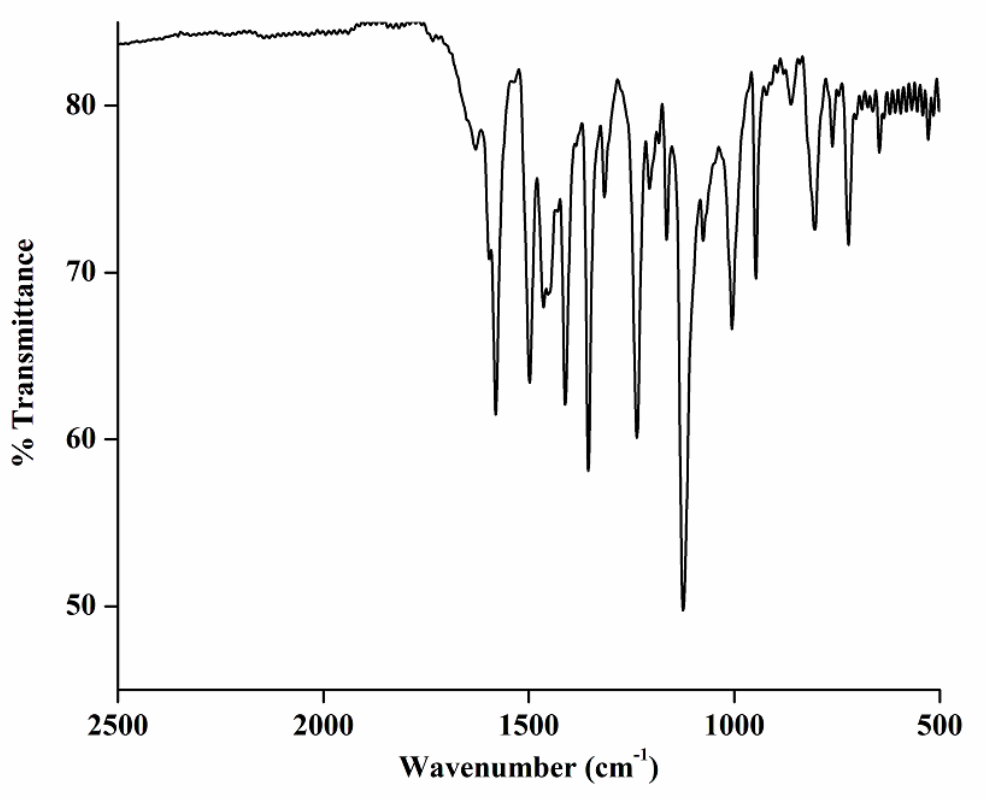

Figure S26. FT-IR spectrum of complex **[(TTMPP^{2-})Mn^{III}(DTC)]** in ATR probe.

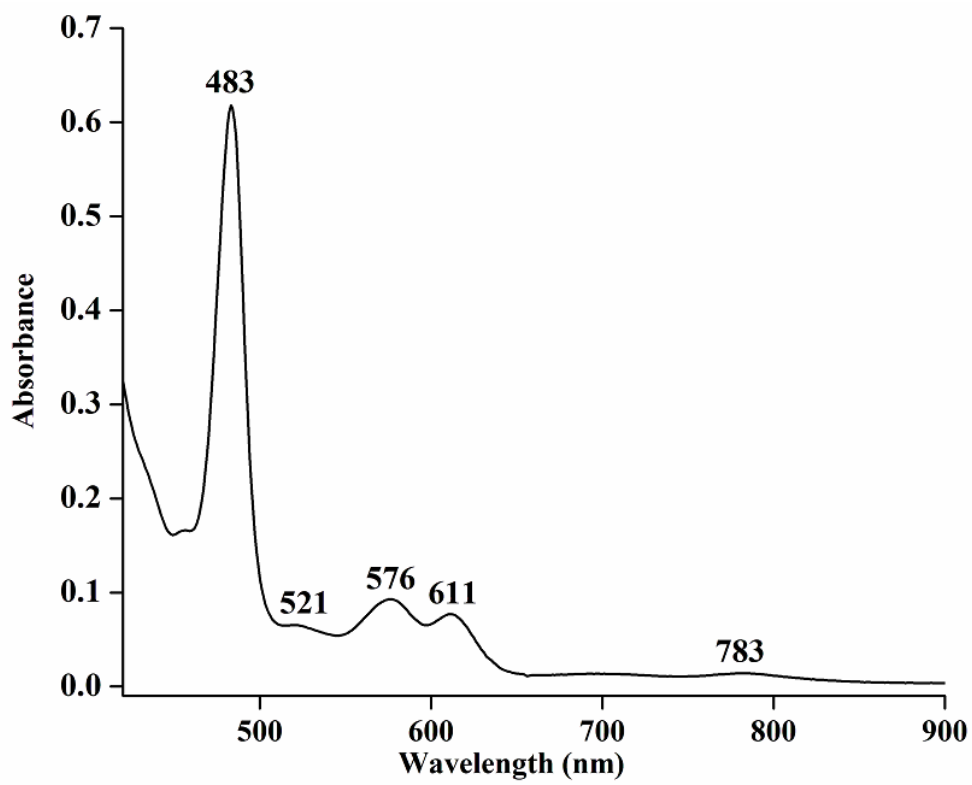

Figure S27. UV-visible spectrum of complex **[(TTMPP^{2-})Mn^{III}(DTC)]** in dichloromethane.

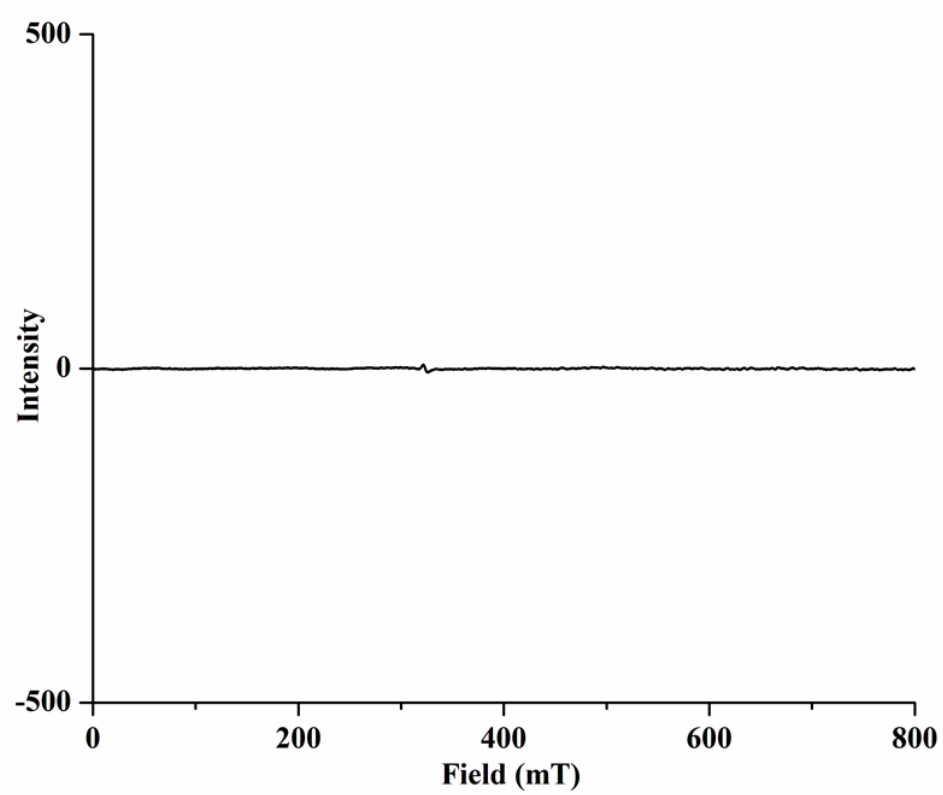

Figure S28. X-band EPR-spectrum of complex **[(TTMPP^{2-})Mn^{III}(DTC)]** in dichloromethane at 77 K.

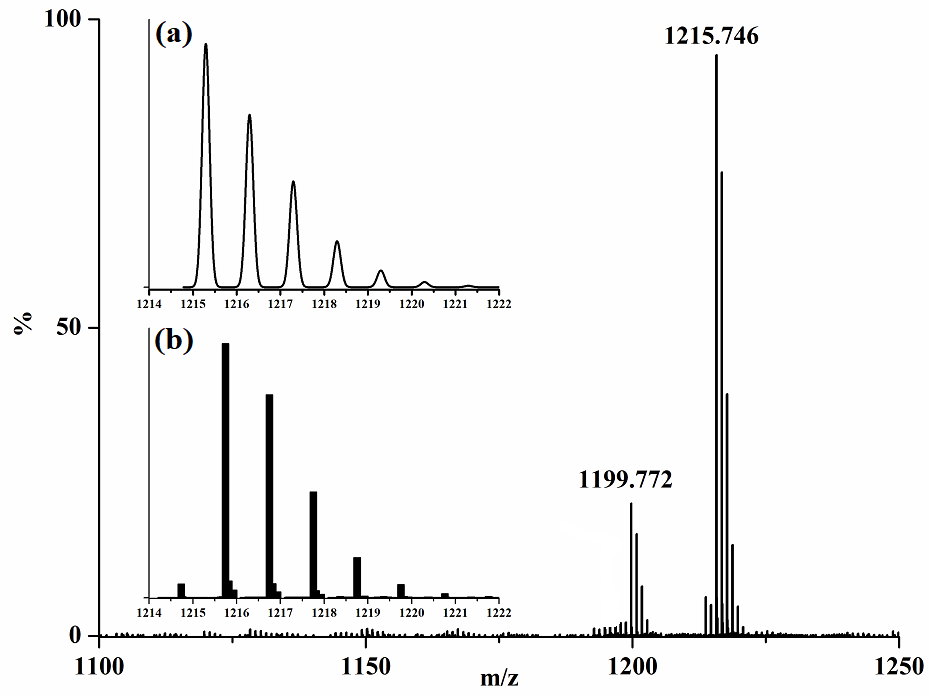

Figure 29. ESI-mass spectrogram of **[(TTMPP^{2-})Mn^{III}(DTC)]** in methanol. [Inset: (a) simulated and (b) experimental isotopic distribution pattern.]

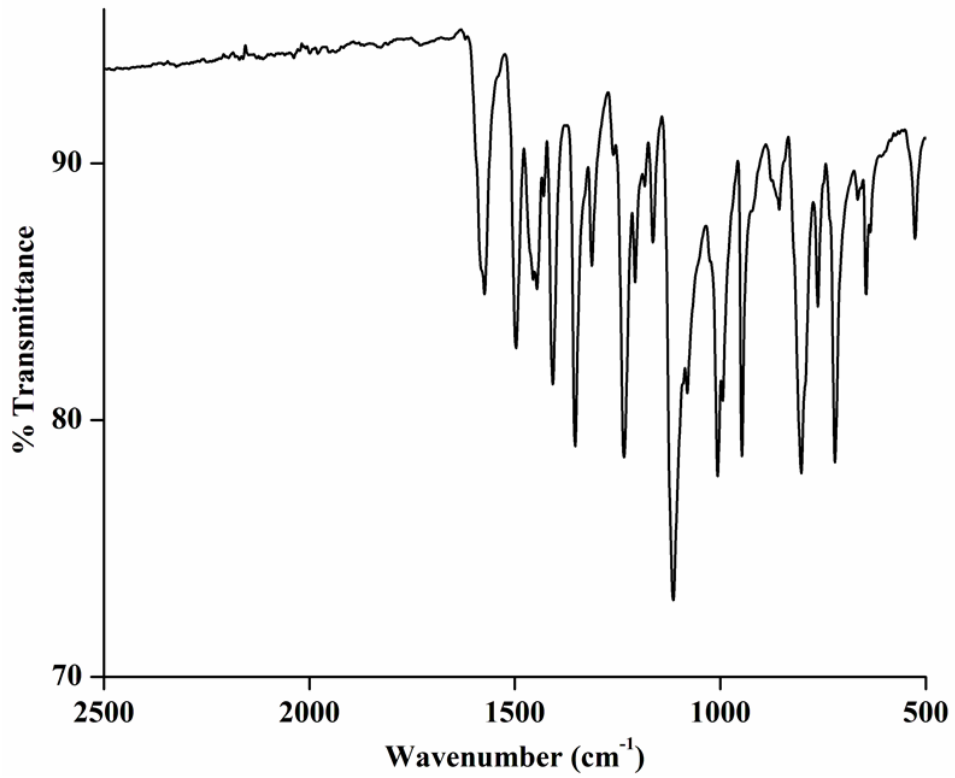

Figure S30. FT-IR spectrum of **[Mn(TTMPP^{2-})Cl]** isolated from reaction mixture in ATR probe.

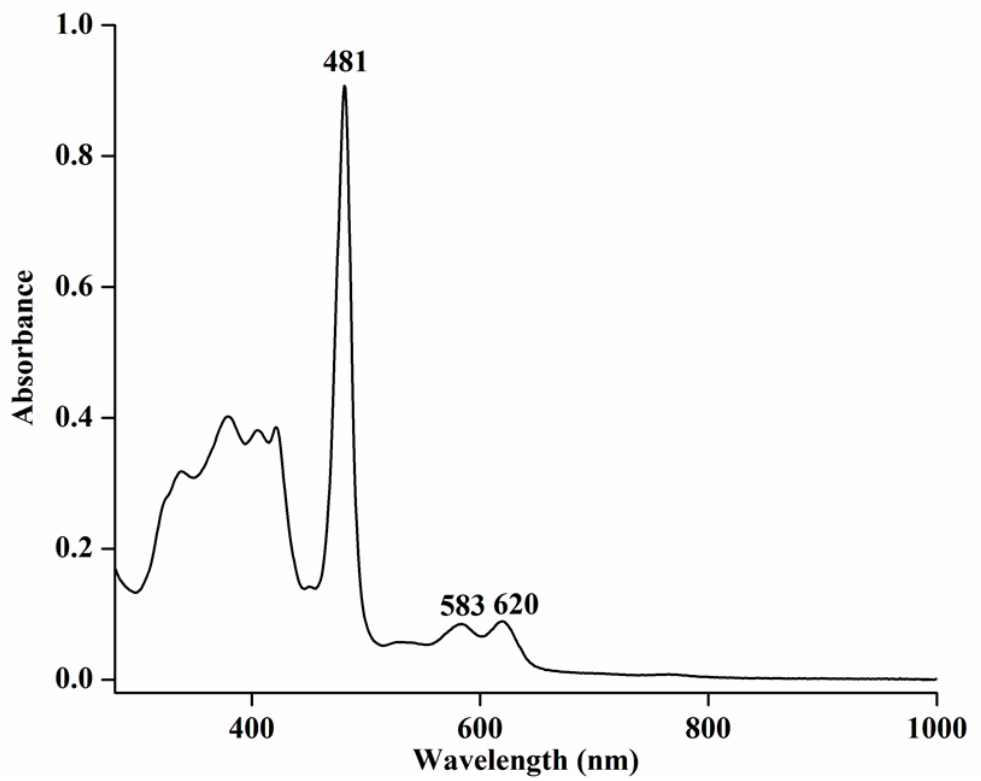

Figure S31. UV-visible spectrum of **[Mn(TTMPP^{2-})Cl]** isolated from reaction mixture in dichloromethane.

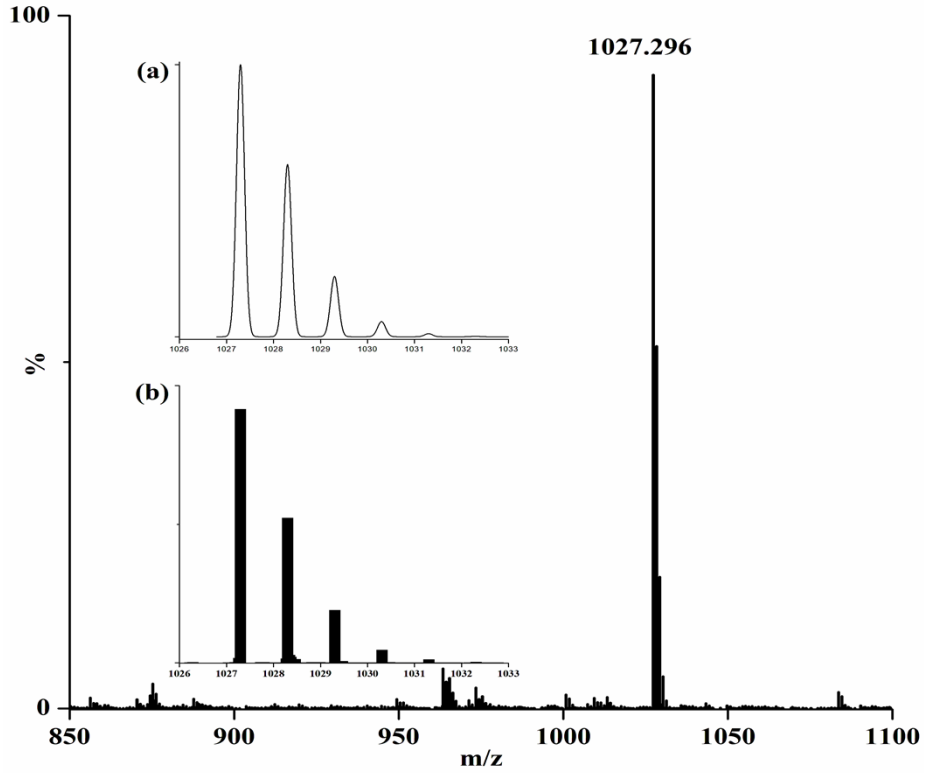

Figure S32. ESI-mass spectrogram of **[Mn(TTMPP^{2-})Cl]** isolated from reaction mixture. [Inset: (a) simulated and (b) experimental isotopic distribution pattern.]

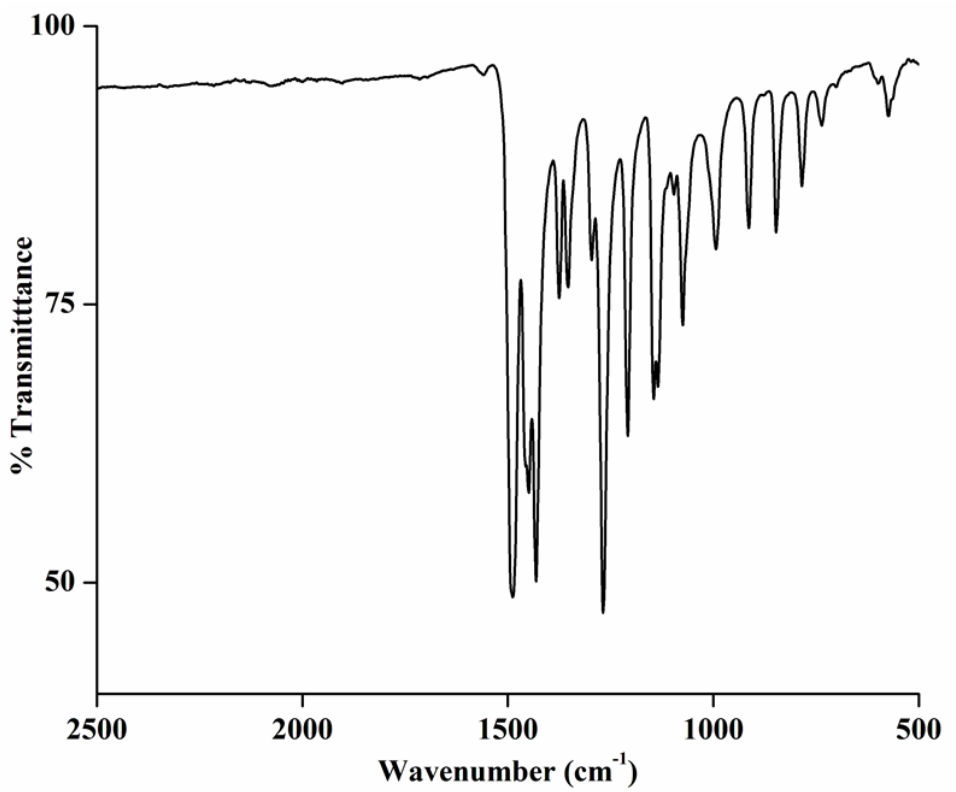

Figure S33. FT-IR spectrum of dichloromethane solution of **[$Fe^{III}(DTC)_3$]** after purging the headspace gas in ATR probe.

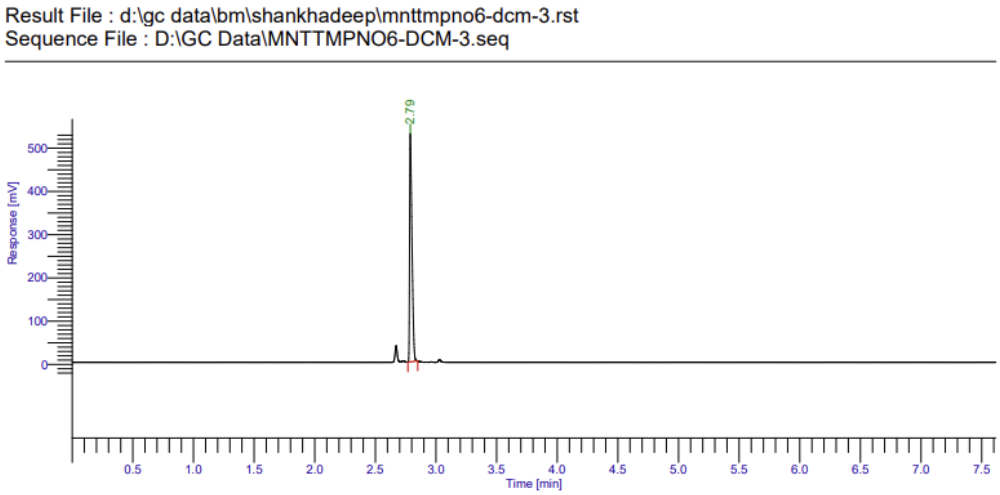

IIT Guwahati Chemistry Dept.

Peak #	Component Name	Time [min]	Area [uV*sec]	Height [uV]	Area [%]
1		2.788	704776.39	527521.17	100.00
			704776.39	527521.17	100.00

Figure S34. Gas chromatogram of standard N2O. (retention time = 2.79 min)

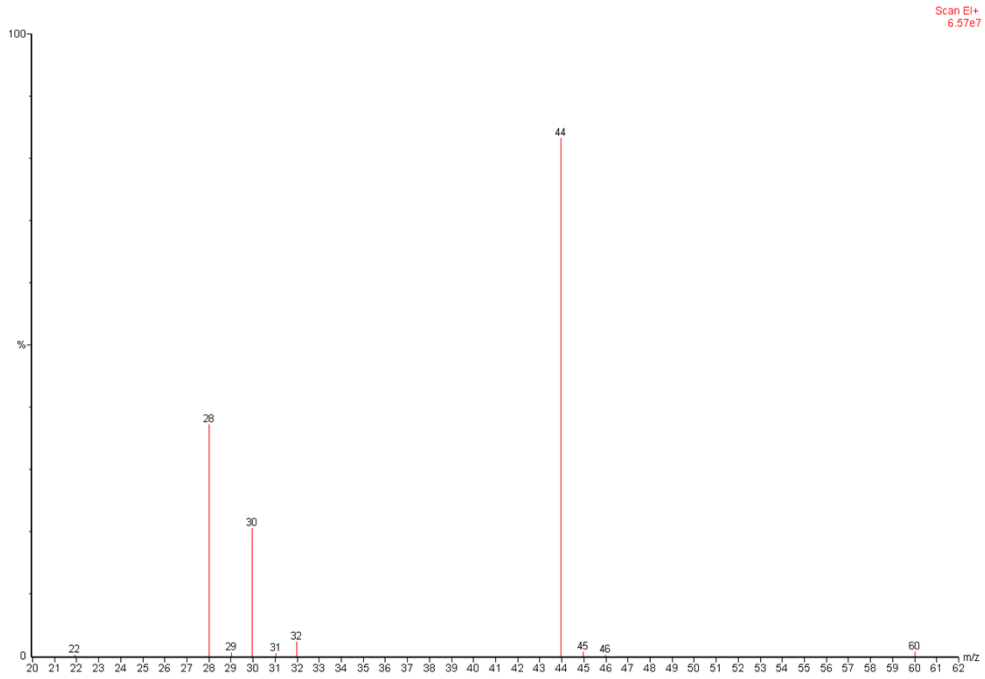

Figure S35. GC-mass spectrum of the headspace gas of the DCM solution of complex **1**.

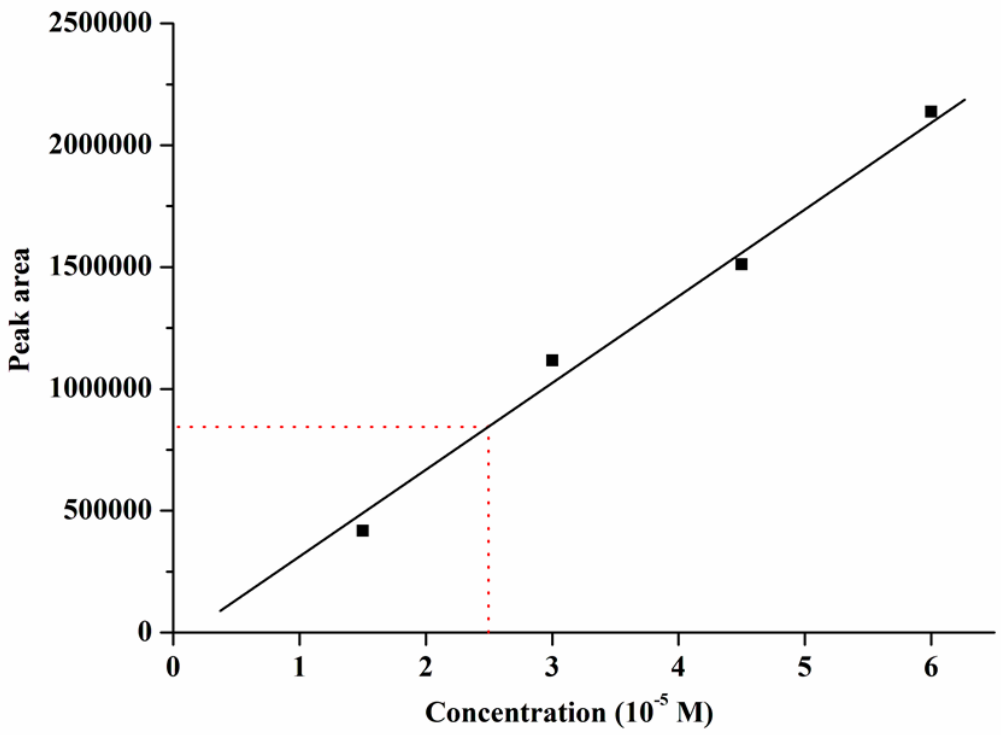

Figure S36. GC calibration curve for determination of the amount of N_2O (red dot corresponds to the sample).

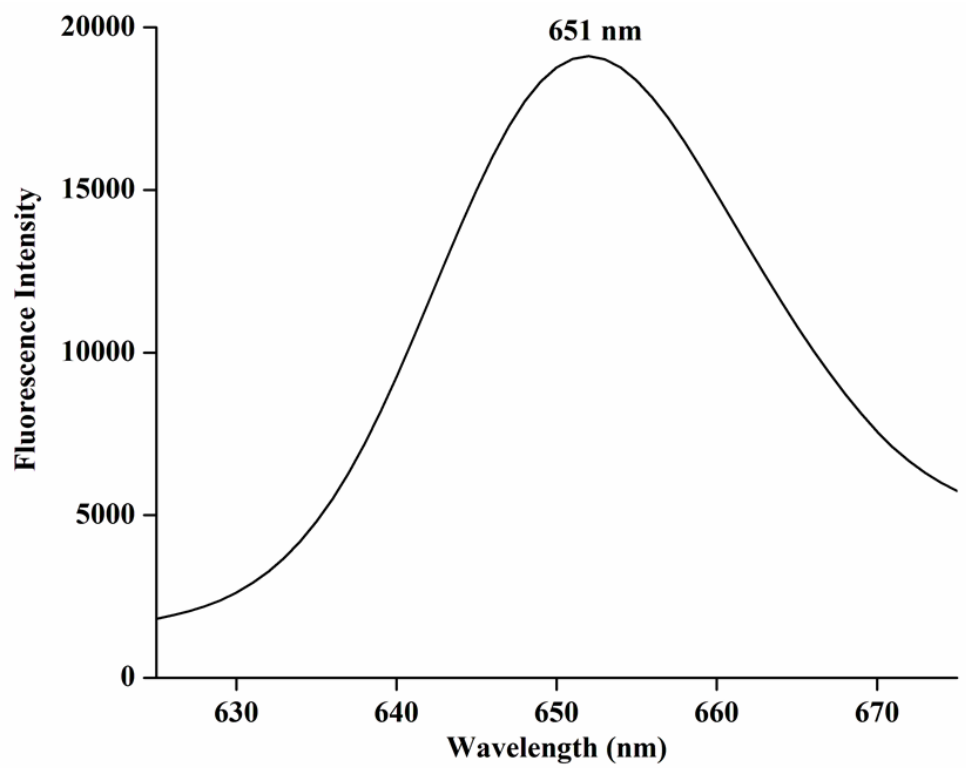

Figure S37. Fluorescence response (λ_{ex} = 420 nm) of complex **1** in dichloromethane solution at 298 K.

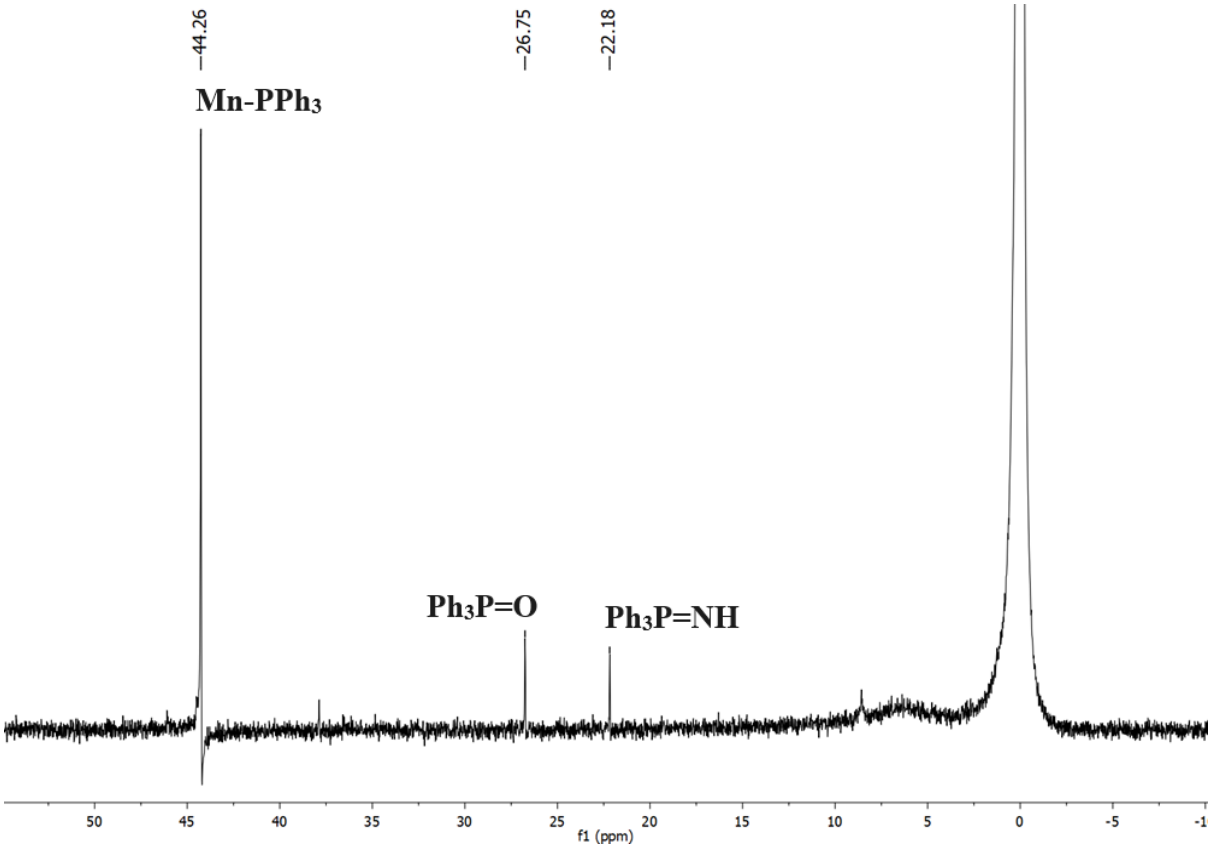

Figure S38. ^{31}P NMR spectrum of the reaction mixture of PPh_3, complex **1** and $HBF_4.Et_2O$ in dichloromethane solution with a few drops of DMSO-d_6.

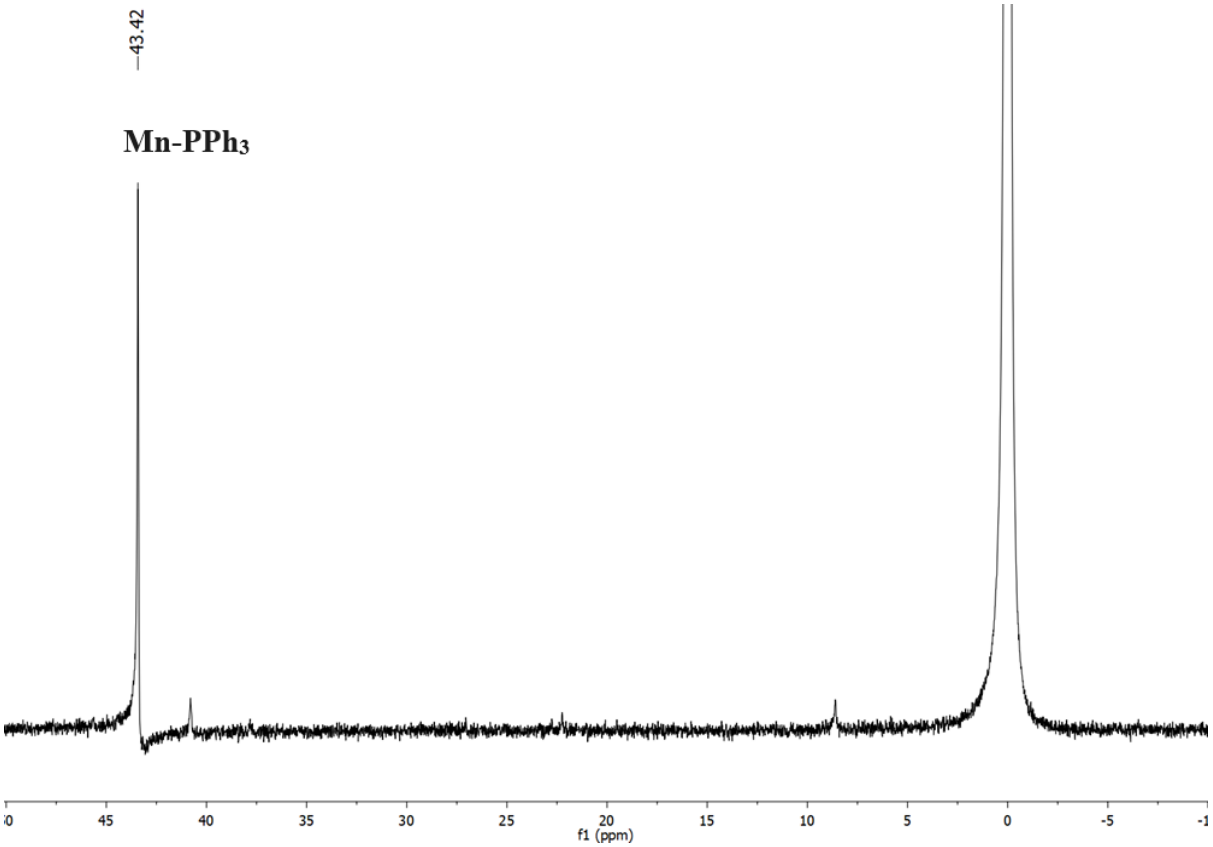

Figure S39. ^{31}P NMR spectrum of the reaction mixture of PPh_3 and complex **1** in the absence of $HBF_4.Et_2O$ in dichloromethane solution with a few drops of DMSO-d_6.

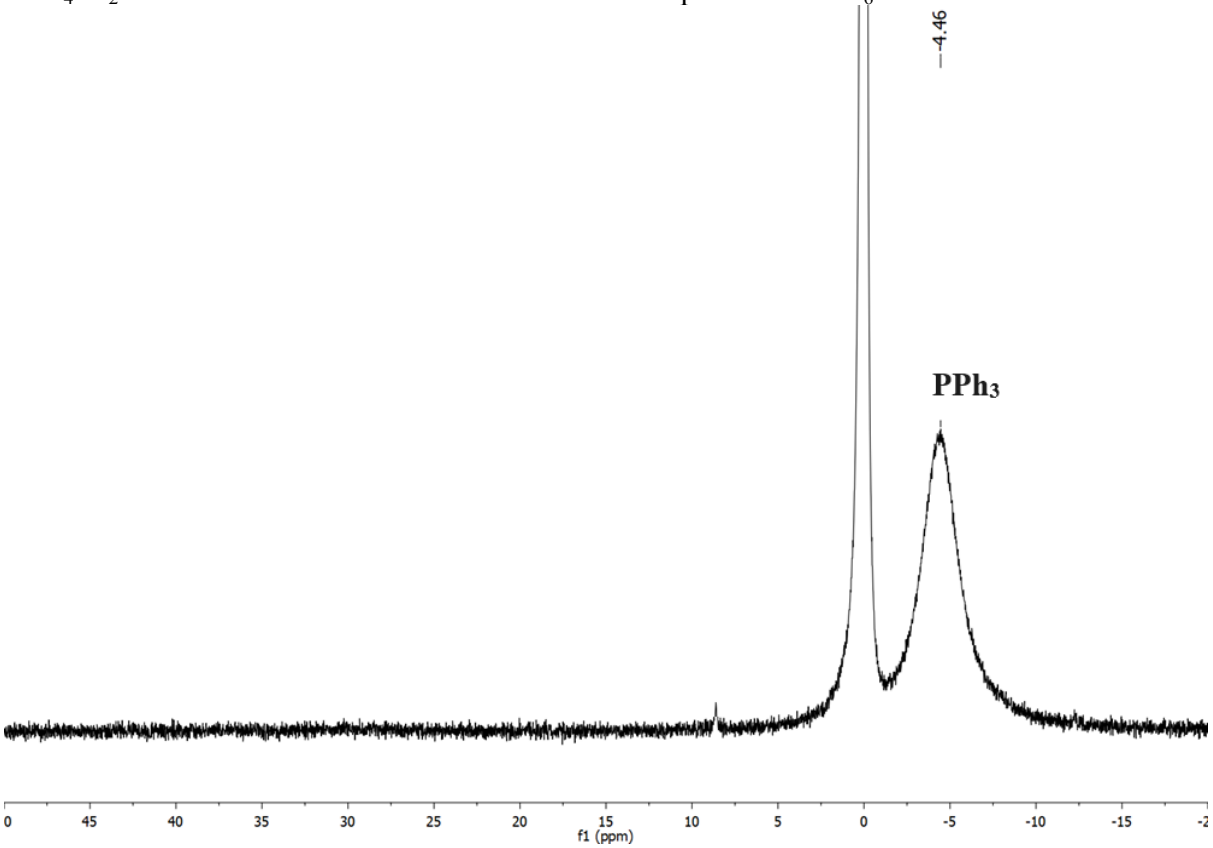

Figure S40. ^{31}P NMR spectrum of the reaction mixture of PPh_3 and complex **1** in the absence of $HBF_4.Et_2O$ and visible light in dichloromethane solution with a few drops of DMSO-d_6.

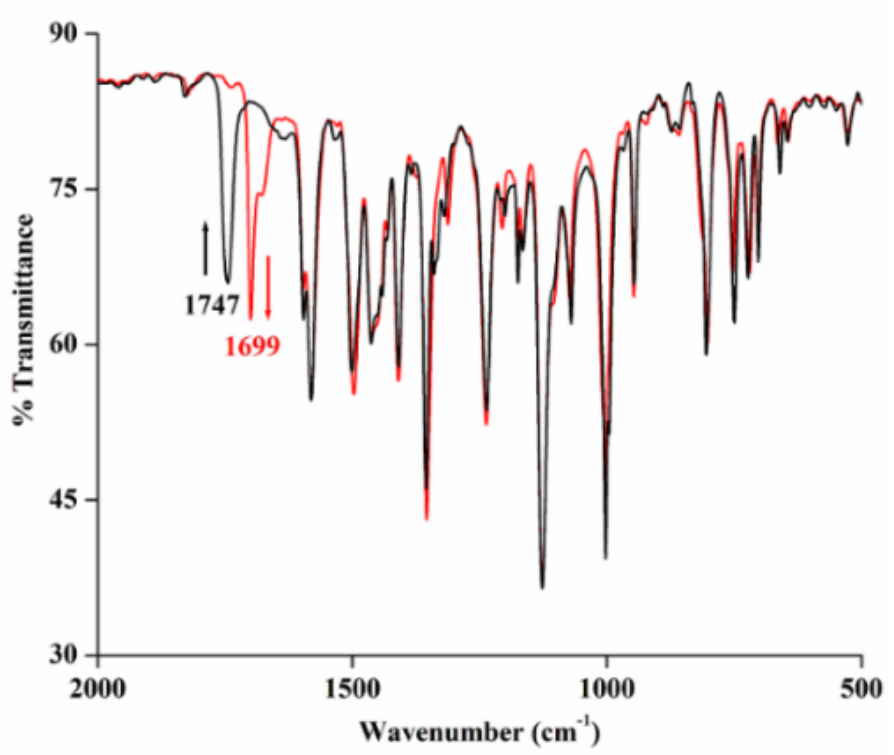

Figure S41a. FT-IR spectrum of the dichloromethane solution of the reaction mixture of complex 1 and [FeIII(TPP)Cl] in ATR Probe [Initial (Black); Final (red)].

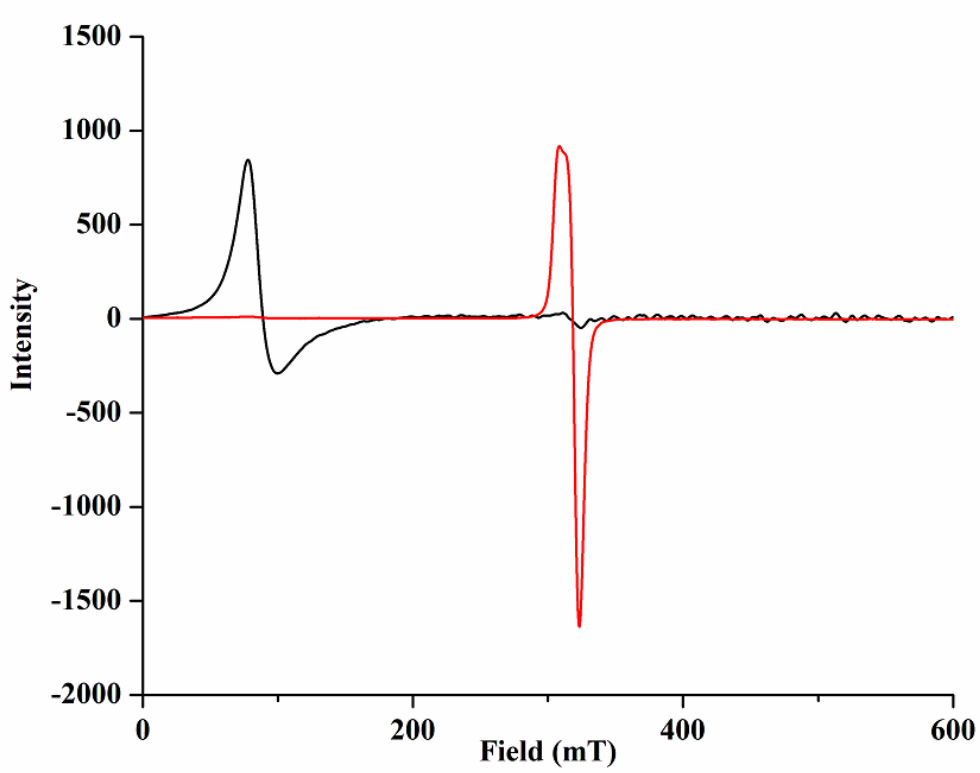

Figure S41b. X-band EPR spectra of the reaction of [Fe^{III}(TPP)Cl] and complex **1** in dichloromethane at 77 K [Initial (black) and final (red)].

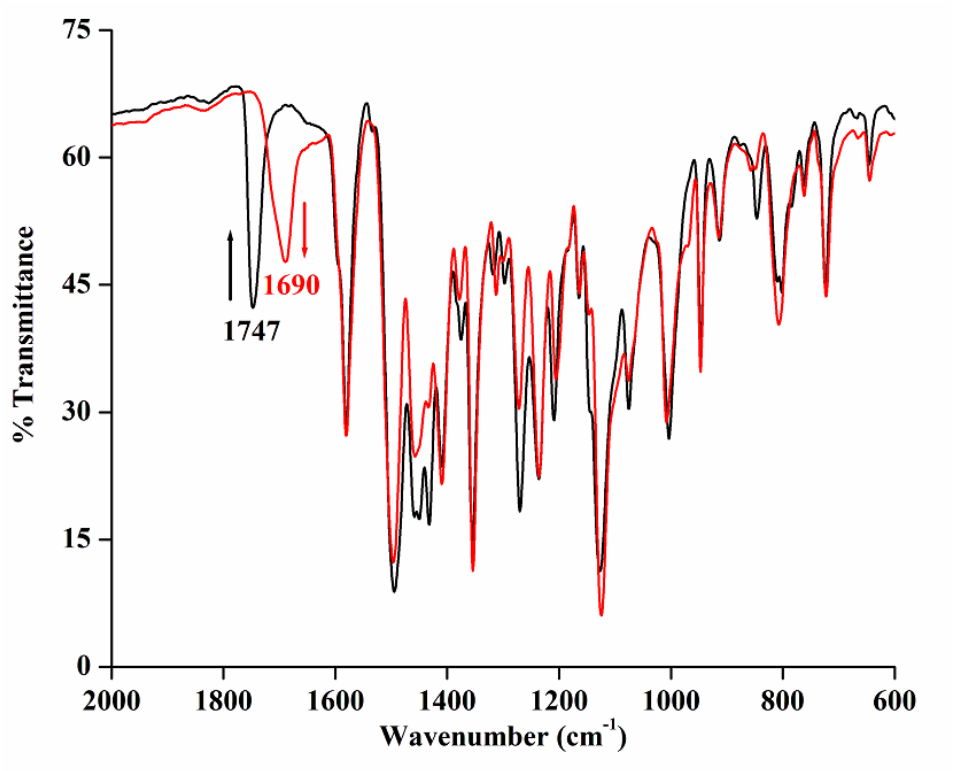

Figure S42. FT-IR spectrum of the dichloromethane solution of reaction mixture of complex **1** and **[Fe(DTC)$_3$]** in ATR probe [Initial (Black); Final (red)].

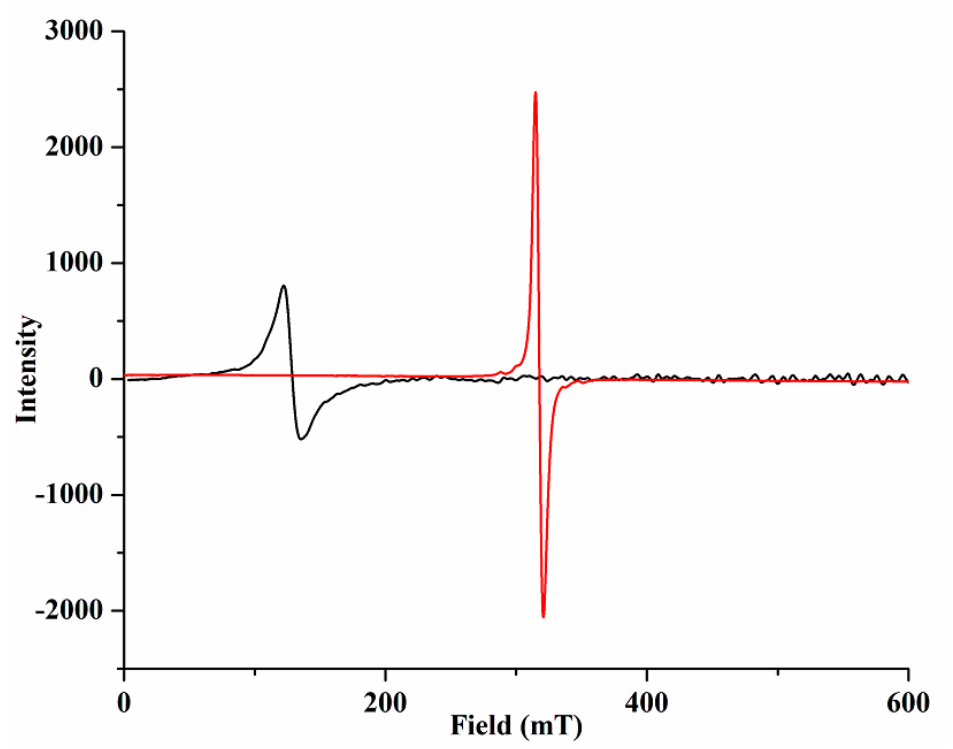

Figure S43. X-band EPR spectra of the Reaction of **[Fe(DTC)$_3$]** and complex **1** in dichloromethane at 77K. [Initial (black) and final (red)].

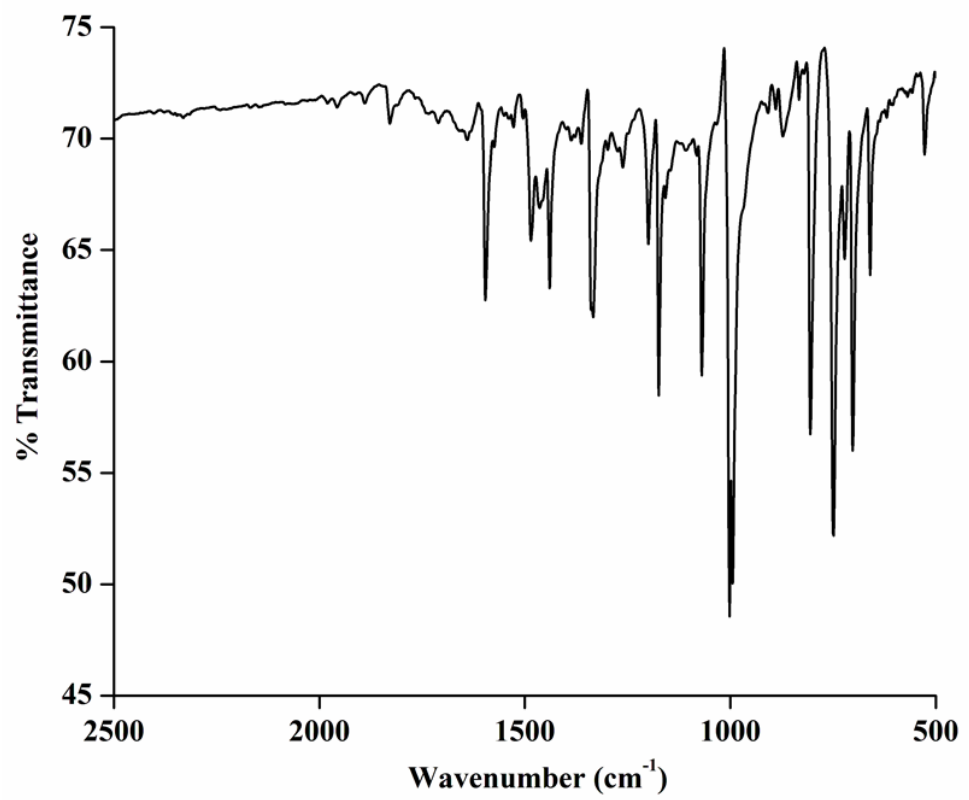

Figure S44. FT-IR spectrum of complex **[Fe(TPP)Cl]** in ATR probe.

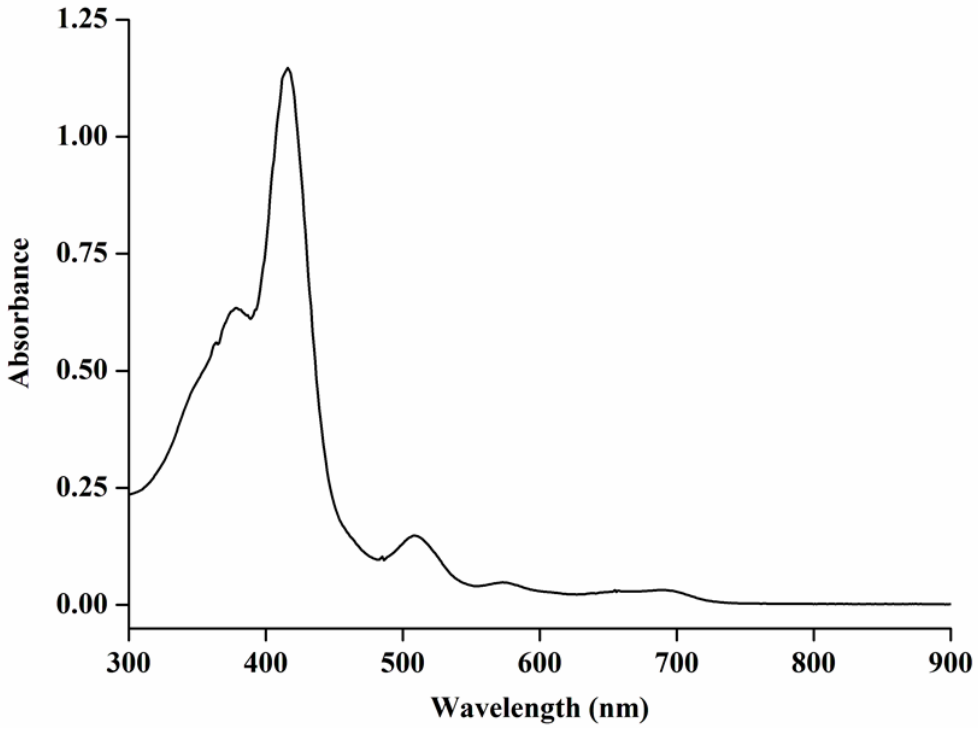

Figure S45. UV-visible spectrum of complex **[Fe(TPP)Cl]** in dichloromethane.

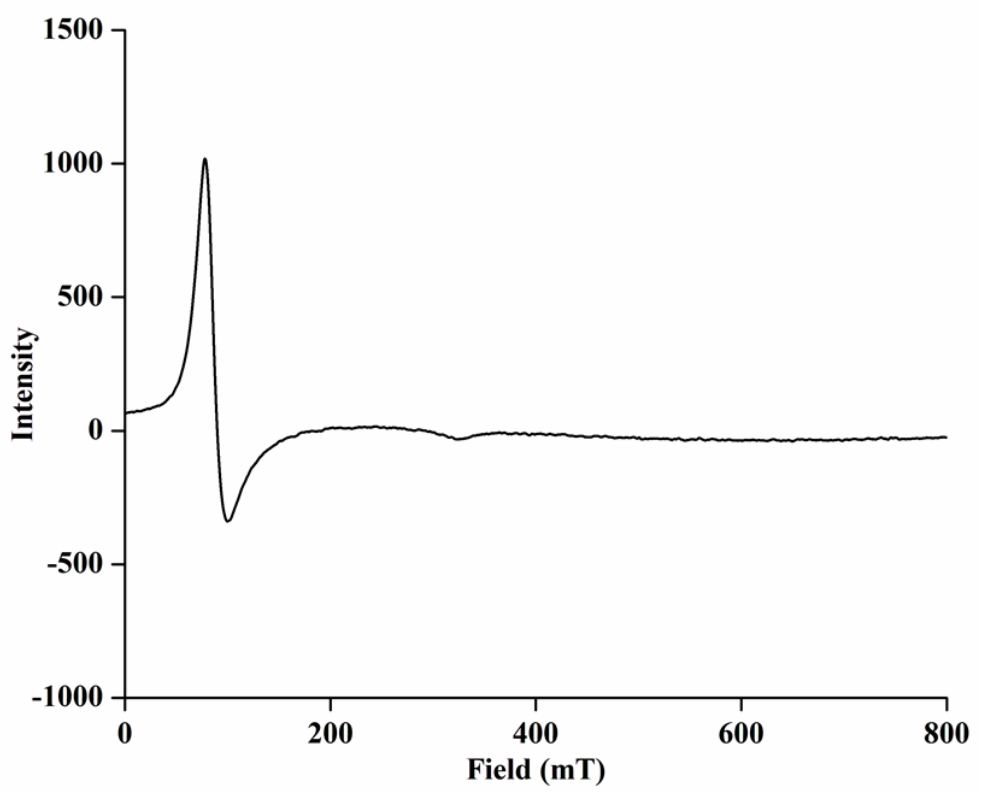

Figure S46. X-band EPR spectra of **[Fe(TPP)Cl]** in dichloromethane at 77 K.

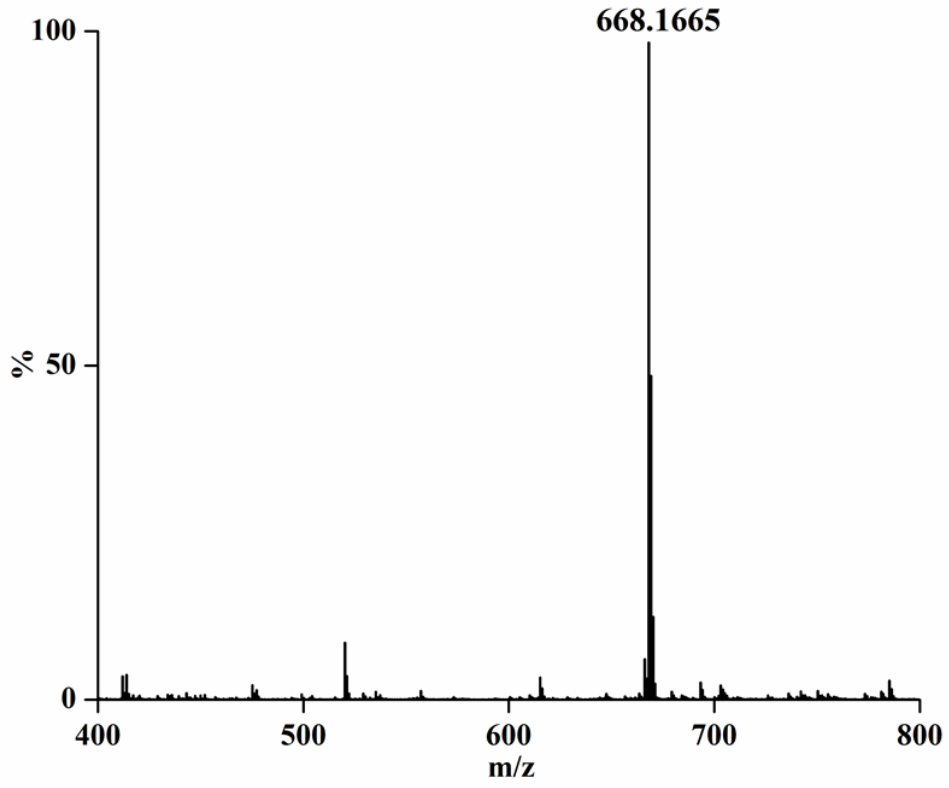

Figure S47. ESI-mass spectrogram of **[Fe(TPP)Cl]** in methanol.

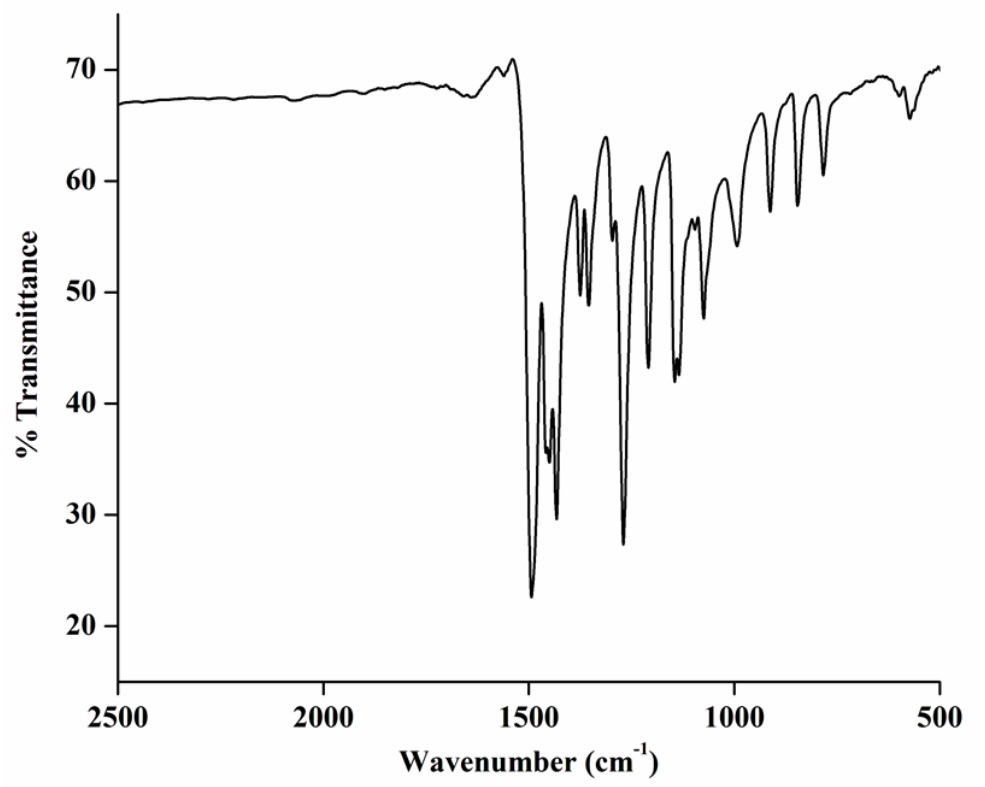

Figure S48. FT-IR spectrum of complex **[Fe(DTC)$_3$]** in ATR probe.

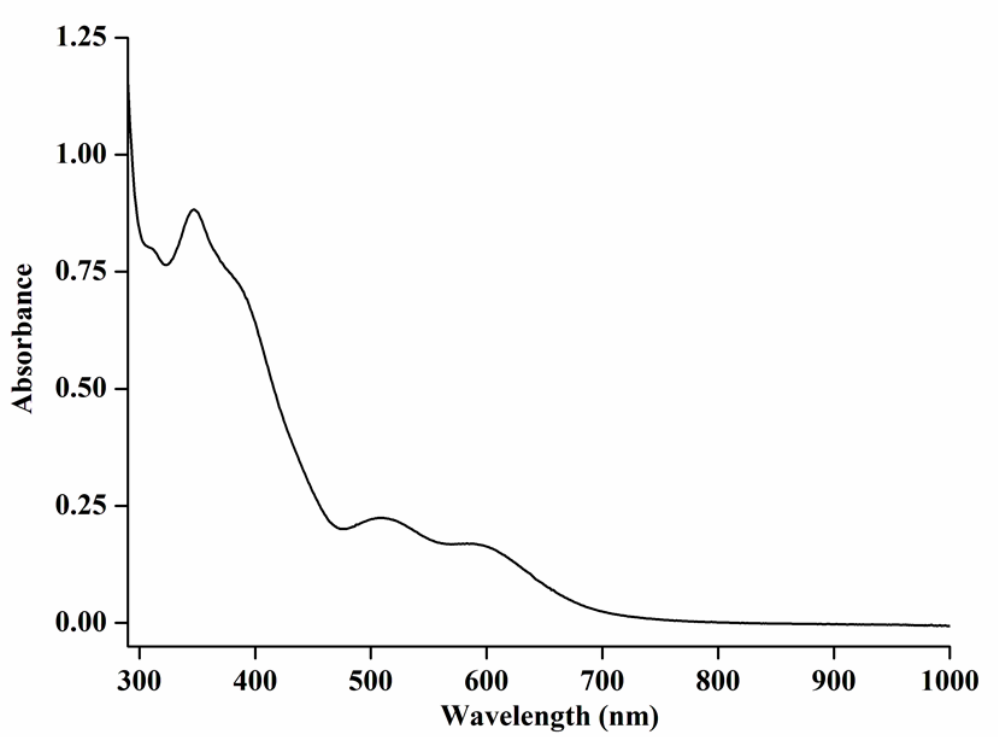

Figure S49. UV-visible spectrum of complex **[Fe(DTC)$_3$]** in dichloromethane.

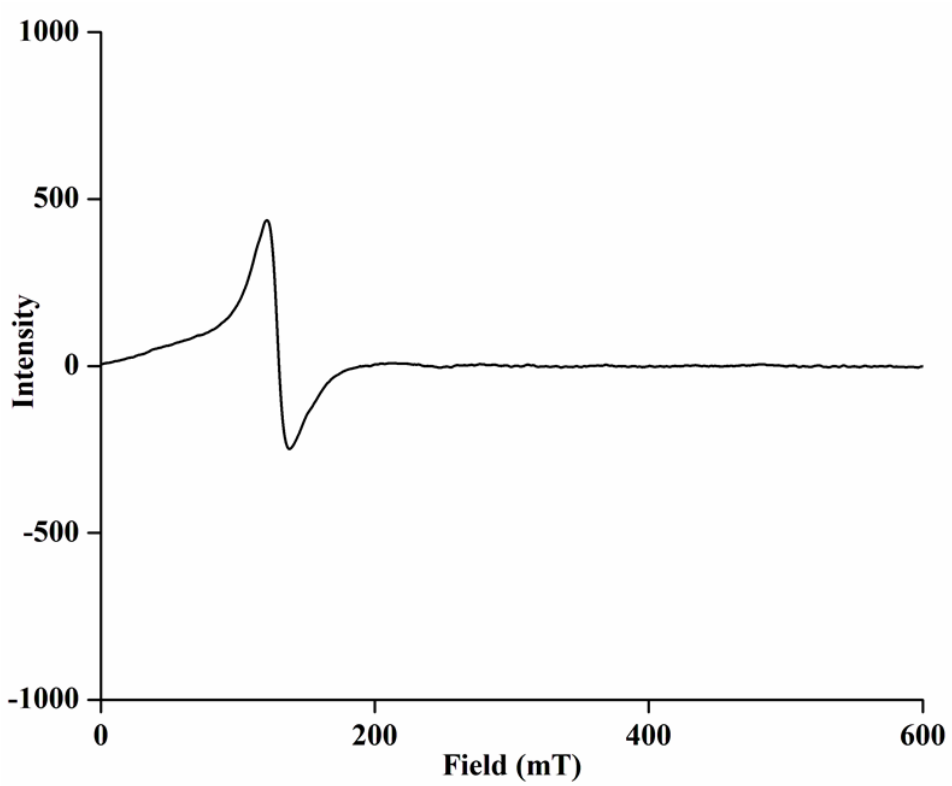

Figure S50. X-band EPR spectra of **[Fe(DTC)$_3$]** in dichloromethane at 77 K.

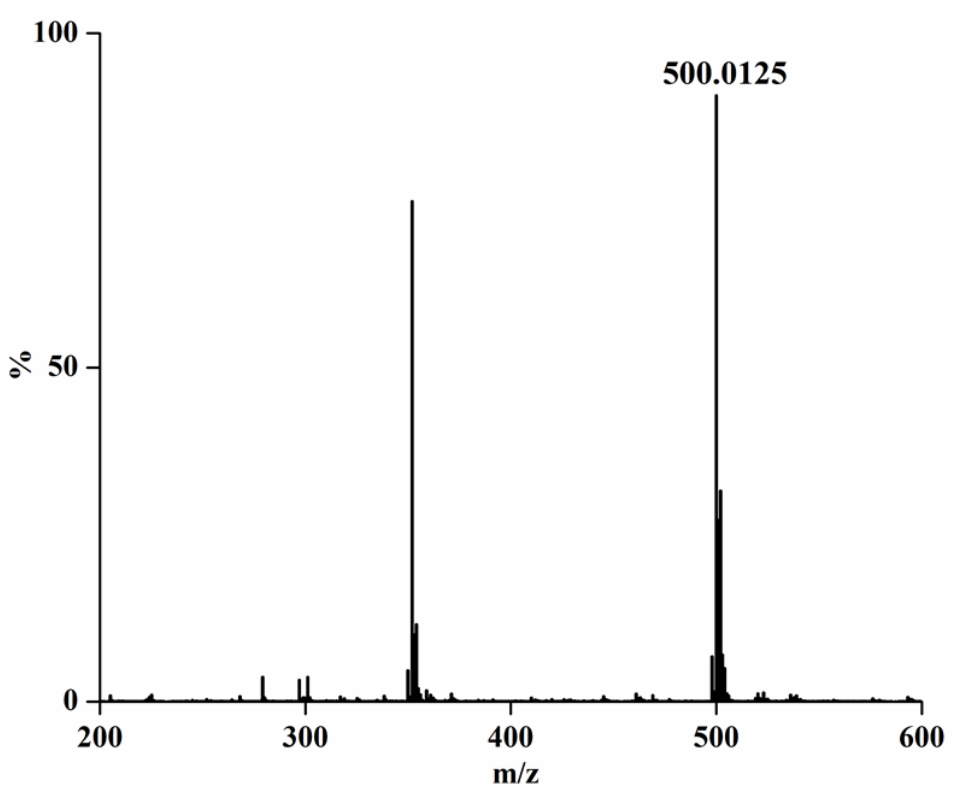

Figure S51. ESI-mass spectrogram of **[Fe(DTC)$_3$]** in methanol.

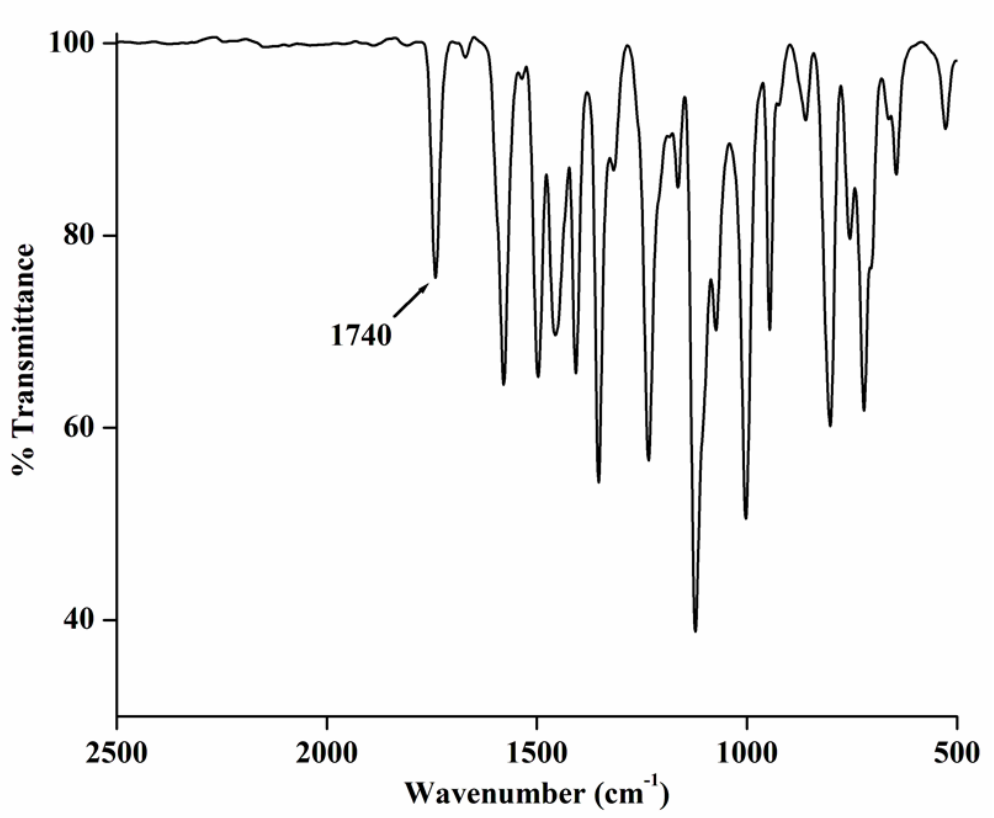

Figure S52. FT-IR spectrum of the dichloromethane solution of the reaction mixture of complex **1** and **[Fe(TPP)Cl]** in the absence of light after 6 hours in ATR probe.

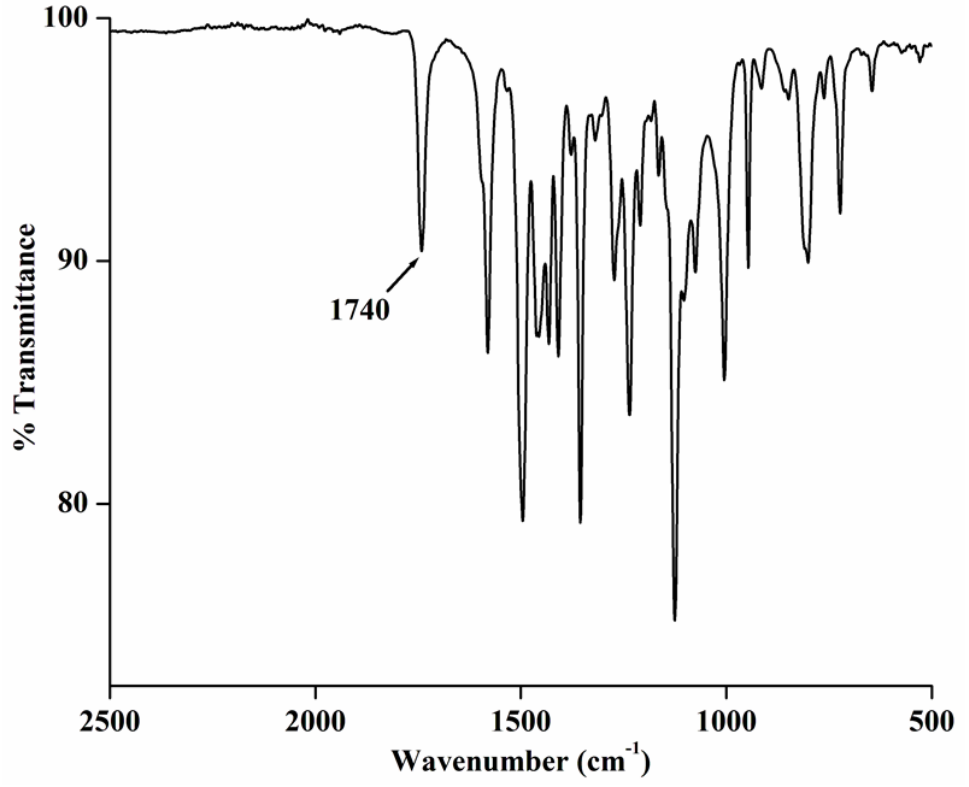

Figure S53. FT-IR spectrum of the dichloromethane solution of the reaction mixture of complex **1** and **[Fe(DTC)$_3$]** in the absence of light after 6 hours in ATR probe.

UV-visible Kinetics Study:

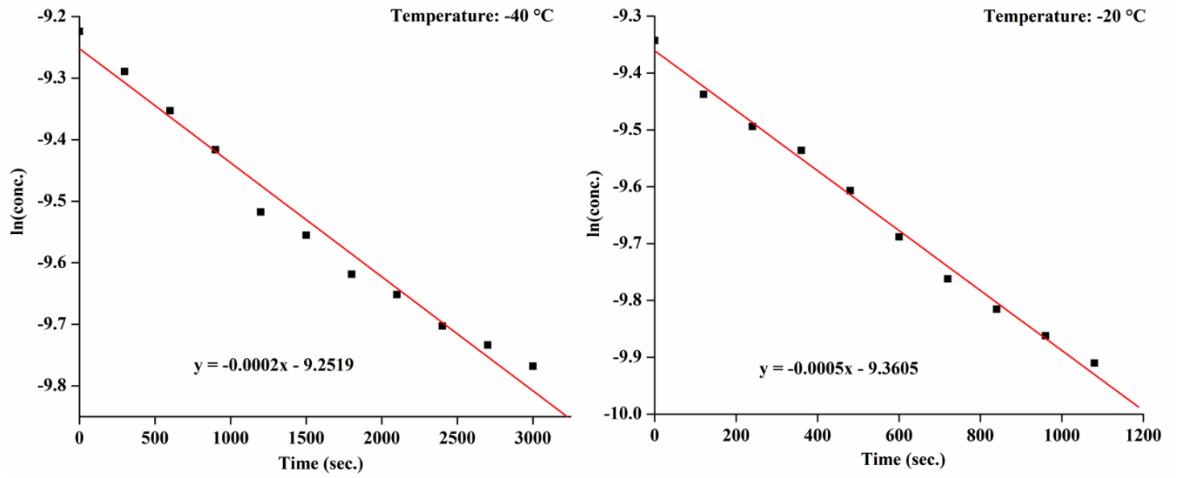

(a) **(b)**

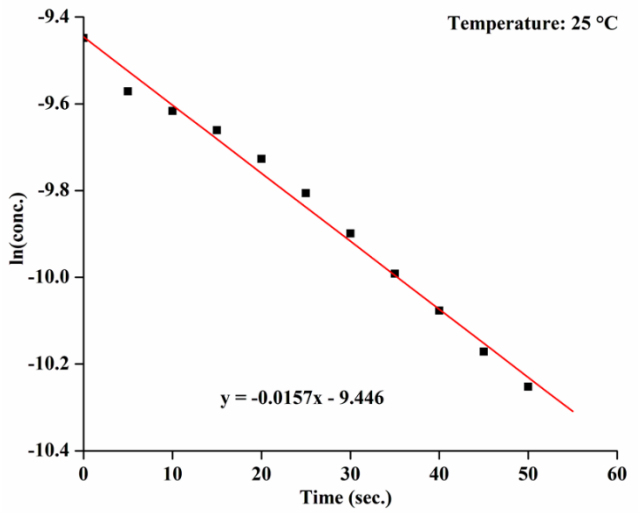

(c)

Temp (K)	Reaction Rate (s^{-1})
233	2×10^{-4}
253	5×10^{-4}
298	157×10^{-4}

Figure S54: UV-visible kinetics of photodecomposition at various temperatures. [(a) -40 °C (233 K) (b) -20 °C (253 K) (c) 25 °C (298 K)]

The photodecomposition of complex **1** was studied in UV-visible spectroscopy at various temperatures and the first order reaction rate was determined. The decomposition rate at 298 K was found to be 79 times faster than that of at – 40 °C.

Table S1. Crystallographic data for complexes.

	1a	**2a**	**2b**
Formulae	$C_{56}H_{52}N_4O_{12}Cl_2Mn$	$C_{56}H_{54}N_4O_{14}Mn$	$C_{83}H_{81}BN_4O_{14}Cl_3Mn$
Mol. wt.	1098.86	1061.97	1530.62
Crystal system	Triclinic	Triclinic	Monoclinic
Space group	P -1	P -1	P 21/c
Temperature /K	298(2)	298.0	297.00
Wavelength /Å	0.71073	0.71073	0.71073
a /Å	8.0273(4)	7.981(3)	15.425(5)
b /Å	12.4667(6)	12.383(5)	22.911(7)
c /Å	14.3129(7)	14.282(6)	25.451(8)
α/°	86.5190(10)	85.706(12)	90
β/°	75.1190(10)	76.649(12)	105.144(9)
γ/°	88.2800(10)	87.299(13)	90
V/ $Å^3$	1381.60(12)	1368.9(9)	8682(5)
Z	1	1	4
Density/Mgm^{-3}	1.321	1.288	1.171
Abs. Coeff. /mm^{-1}	0.400	0.309	0.304
Abs. correction	none	none	none
F(000)	571	555	3200
Total no. of reflections	4862	6126	19273
Reflections, $I > 2\sigma(I)$	4109	4129	12494
Max. 2θ/°	25.000	25.242	25.242
Ranges (h, k, l)	$-9 \le h \le 9$ $-14 \le k \le 14$ $-17 \le l \le 17$	$-10 \le h \le 10$ $-15 \le k \le 15$ $-18 \le l \le 18$	$-19 \le h \le 19$ $-29 \le k \le 29$ $-32 \le l \le 32$
Complete to 2θ (%)	0.998	0.976	0.995
Refinement method	Full-matrix least-squares on F^2	Full-matrix least-squares on F^2	Full-matrix least-squares on F^2
Goof (F^2)	1.053	1.059	1.073
R indices [$I > 2\sigma(I)$]	0.0615	0.0728	0.0960
R indices (all data)	0.0741	0.1118	0.1420

Table S2. Selected bond lengths (Å) of complex **1**.

Atoms	1a	2a	2b
Mn1-N1	2.011(2)	2.011(2)	2.008(3)
Mn1-N2	2.007(2)	1.992(3)	2.002(3)
Mn1-N3	-	-	2.003(3)
Mn1-N4	-	-	2.008(3)
Mn1-Cl1	2.5277(17)		-
Mn1-O7	-	2.098(5)	-
Mn1-O13	-	-	2.270(3)
Mn1-O14	-	-	2.261(3)

Table S3. Selected bond angles (˚) of complex **1**.

Atoms	1a	2a	2b
N1-Mn1-N2	90.86(10)	89.01(10)	90.03(13)
N1-Mn1-Cl1	90.26(9)	-	-
N2-Mn1-Cl1	89.46(9)	-	-
N1-Mn1-O7	-	90.05(12)	-
N2-Mn1-O7	-	88.44(12)	-
N2-Mn1-N3			89.74(13)
N3-Mn1-N4			89.86(13)
N4-Mn1-N1			90.36(13)

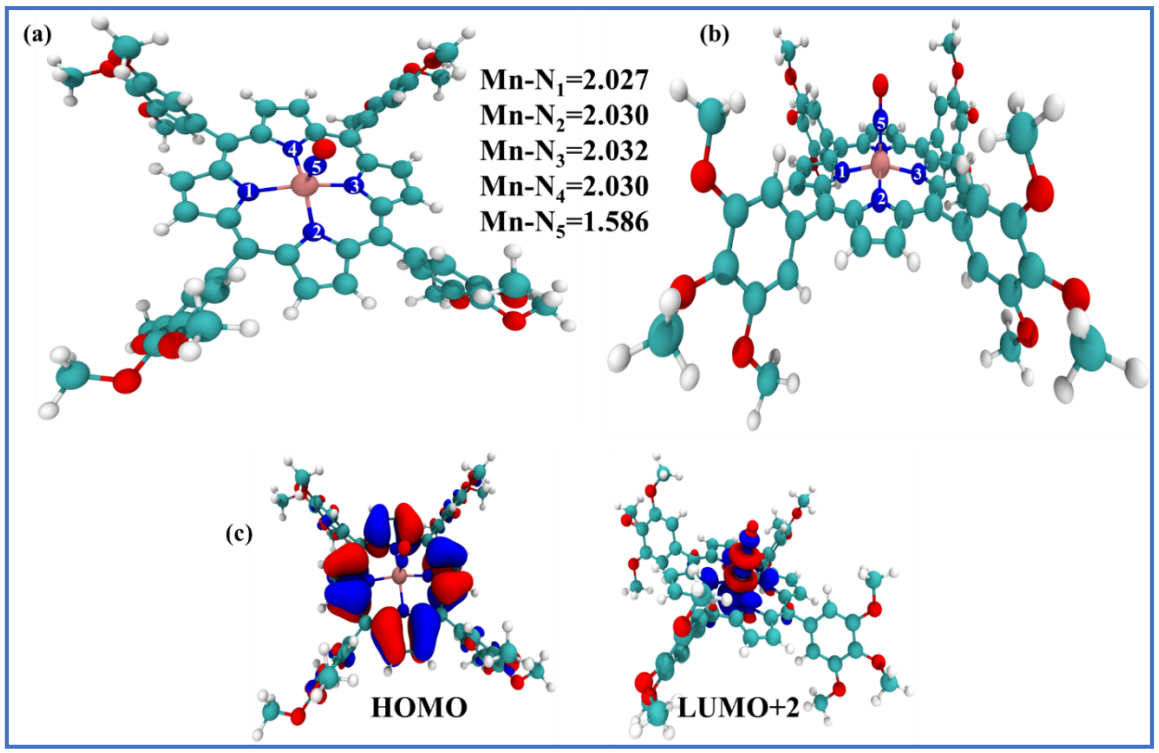

Figure S55. Optimized structure of Mn-Porphyrin systems with NO binding: (a) top view, (b) side view. Mn-N distances are indicated in Angstrom (Å). (c) HOMO and LUMO+2 orbitals of the optimized structure.

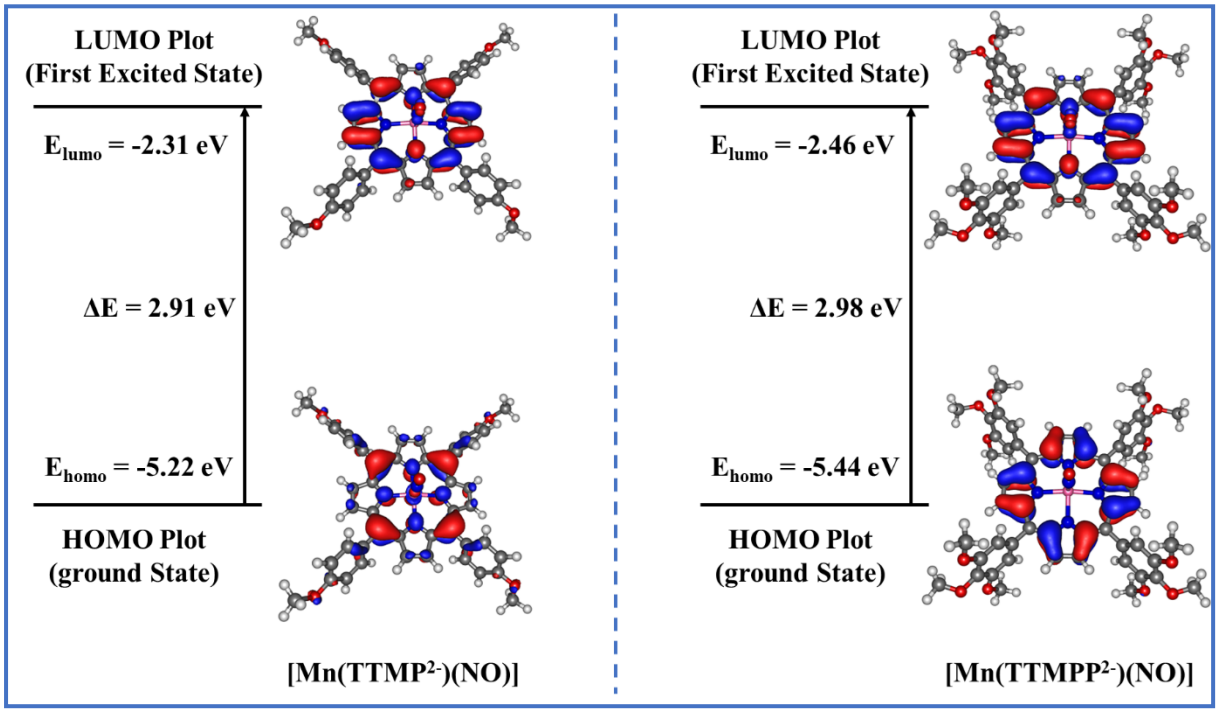

Figure S56. HOMO–LUMO energy gap of [Mn(TTMP^{2-})(NO)] and [Mn(TTMPP^{2-})(NO)], **1** at LC-BLYP and ω-B97XD methods respectively.

Cartesian coordinates of the optimized geometry of [Mn(TTMPP^{2-})(NO)].

Mn	-0.000034000	-0.001739000	-0.242167000
N	0.000009000	-2.011752000	0.057420000
N	-2.003195000	-0.008335000	0.087777000
O	-5.928410000	-5.024330000	-2.349619000
O	5.147037000	-6.003362000	2.159715000
O	-5.146208000	-6.002720000	2.162768000
O	-6.400069000	-6.500650000	-0.147273000
O	6.400447000	-6.500106000	-0.150793000
O	5.928058000	-5.022899000	-2.352437000
C	2.840340000	-1.108989000	0.068674000
C	-2.840384000	-1.109069000	0.069127000
C	1.100078000	-2.849890000	0.028434000
C	4.220280000	-0.691008000	0.112759000
H	5.066677000	-1.361547000	0.124789000
C	-3.497168000	-3.502350000	-0.011001000
C	-3.783676000	-4.250110000	1.135852000
H	-3.231210000	-4.048563000	2.044559000
C	4.199065000	-3.730462000	-1.201049000
H	3.958422000	-3.138244000	-2.074533000
C	2.436695000	-2.445559000	0.029648000
C	3.497237000	-3.502189000	-0.012551000
C	-5.189600000	-4.722105000	-1.243062000
C	-2.436686000	-2.445629000	0.030514000
C	-4.199245000	-3.731226000	-1.199234000
H	-3.958864000	-3.139379000	-2.073042000
C	4.781709000	-5.235746000	1.094127000
C	4.221498000	0.669397000	0.139356000
H	5.069462000	1.337083000	0.172767000
C	3.784090000	-4.250434000	1.133899000
H	3.231816000	-4.049351000	2.042824000
C	-1.100053000	-2.849911000	0.028942000
C	5.189508000	-4.721219000	-1.245553000
C	-4.781191000	-5.235552000	1.096750000
C	0.680256000	-4.229414000	-0.018339000
H	1.349005000	-5.076577000	-0.053298000
C	-5.483822000	-5.483270000	-0.096643000
C	5.484101000	-5.482849000	-0.099536000
C	-0.680223000	-4.229427000	-0.017972000
H	-1.348972000	-5.076605000	-0.052572000
C	4.452668000	-5.827668000	3.389070000
H	4.583730000	-4.811645000	3.783960000
H	4.894397000	-6.545273000	4.081743000
H	3.381511000	-6.040371000	3.278868000
C	-4.451433000	-5.826550000	3.391827000
H	-3.380295000	-6.039192000	3.281326000
H	-4.892863000	-6.543959000	4.084894000
H	-4.582454000	-4.810407000	3.786419000
C	-7.767314000	-6.080857000	-0.058501000

H	-7.953397000	-5.571481000	0.895682000
H	-8.369295000	-6.990389000	-0.109147000
H	-8.027768000	-5.420360000	-0.893644000
C	5.655943000	-4.319600000	-3.560350000
H	4.621941000	-4.478815000	-3.891114000
H	6.341159000	-4.732154000	-4.301967000
H	5.842331000	-3.243614000	-3.449437000
C	-5.656639000	-4.321564000	-3.557919000
H	-5.843091000	-3.245543000	-3.447456000
H	-6.341998000	-4.734514000	-4.299183000
H	-4.622703000	-4.480845000	-3.888856000
C	7.767696000	-6.080201000	-0.062591000
H	8.027712000	-5.419555000	-0.897748000
H	8.369727000	-6.989676000	-0.113645000
H	7.954170000	-5.570956000	0.891587000
N	-0.000076000	1.992906000	0.121235000
N	2.003108000	-0.008299000	0.087784000
O	5.948454000	5.036615000	2.487865000
O	-5.075040000	6.008528000	-2.011728000
O	5.075685000	6.009175000	-2.008809000
O	6.364812000	6.518984000	0.280431000
O	-6.364897000	6.519102000	0.276945000
O	-5.949333000	5.037425000	2.484955000
C	-2.841995000	1.090862000	0.126814000
C	2.841863000	1.090914000	0.127388000
C	-1.100192000	2.829487000	0.174852000
C	-4.221616000	0.669301000	0.138840000
H	-5.069610000	1.336970000	0.171852000
C	3.492468000	3.489590000	0.191177000
C	3.750645000	4.241638000	-0.959573000
H	3.183655000	4.035219000	-1.858162000
C	-4.212626000	3.726234000	1.365724000
H	-3.993651000	3.132643000	2.243964000
C	-2.437552000	2.427283000	0.158686000
C	-3.492642000	3.489577000	0.189574000
C	5.192652000	4.727087000	1.394465000
C	2.437382000	2.427314000	0.159611000
C	4.212088000	3.725835000	1.367632000
H	3.992806000	3.131972000	2.245612000
C	-4.737622000	5.237410000	-0.939947000
C	-4.220342000	-0.691118000	0.112966000
H	-5.066714000	-1.361683000	0.125290000
C	-3.750409000	4.241265000	-0.961503000
H	-3.183120000	4.034544000	-1.859835000
C	1.100011000	2.829498000	0.175367000
C	-5.193168000	4.727527000	1.391914000
C	4.737886000	5.237741000	-0.937378000
C	-0.680340000	4.205069000	0.289437000
H	-1.349426000	5.048224000	0.376775000
C	5.458340000	5.492258000	0.243898000

C	-5.458442000	5.492339000	0.241015000
C	0.680087000	4.205071000	0.289788000
H	1.349115000	5.048235000	0.377467000
C	-4.361834000	5.822896000	-3.229347000
H	-4.497828000	4.807840000	-3.624709000
H	-4.783686000	6.544474000	-3.930178000
H	-3.290461000	6.023551000	-3.101078000
C	4.362694000	5.824130000	-3.226642000
H	3.291307000	6.024785000	-3.098483000
H	4.784720000	6.545994000	-3.927073000
H	4.498706000	4.809244000	-3.622437000
C	7.733337000	6.113612000	0.153091000
H	7.899928000	5.613874000	-0.809696000
H	8.327694000	7.028532000	0.196202000
H	8.021318000	5.448835000	0.975835000
C	-5.709482000	4.330103000	3.696733000
H	-4.680609000	4.477486000	4.048705000
H	-6.404816000	4.749249000	4.425171000
H	-5.905462000	3.256228000	3.580933000
C	5.708116000	4.328968000	3.699357000
H	5.904093000	3.255117000	3.583333000
H	6.403196000	4.747881000	4.428171000
H	4.679118000	4.476300000	4.050982000
C	-7.733358000	6.113728000	0.148930000
H	-8.021772000	5.449052000	0.971607000
H	-8.327734000	7.028656000	0.191621000
H	-7.899449000	5.613872000	-0.813882000
N	-0.000042000	0.021054000	-1.840491000
O	-0.000076000	0.042523000	-3.019390000

Cartesian coordinates of the optimized geometry of [Mn(TTMP^{2-})(NO)].

Mn	-0.010163	-0.017757	0.190542
N	1.980995	0.017543	-0.189899
N	-2.013152	-0.040777	-0.121992
N	-0.044082	1.995113	-0.087960
C	4.524151	5.426605	-1.206660
H	4.619407	6.123395	-2.033043
C	5.413227	5.538716	-0.126517
O	-6.619380	6.281107	0.160743
N	0.012833	-2.019252	-0.160554
C	1.045384	2.845535	-0.035300
O	6.516607	-6.377396	-0.482443
C	-2.486781	2.392073	-0.067506
C	2.797656	1.131760	-0.261786
C	-1.074642	-2.871877	-0.100691
O	-6.370252	-6.563937	-0.227161
C	4.166617	0.734812	-0.482171
H	4.993433	1.415752	-0.617769

C	3.668603	-4.312926	-1.380255
H	2.979958	-4.219508	-2.214772
C	3.548540	4.436408	-1.206219
H	2.865343	4.355461	-2.046503
C	3.432374	3.529122	-0.137811
C	5.568188	-5.402146	-0.349191
C	-1.155680	2.813797	-0.002402
C	-4.208243	-0.748286	-0.362300
H	-5.040056	-1.424276	-0.491796
C	2.828772	-1.069452	-0.305918
C	-0.752900	4.191507	0.139545
H	-1.428751	5.026455	0.247541
C	-3.564227	3.426835	-0.034947
O	6.333643	6.545133	-0.218425
C	-2.417588	-2.486439	-0.145899
C	-4.227281	0.612049	-0.341446
H	-5.078047	1.267927	-0.450002
C	3.531103	-3.450901	-0.277453
C	-3.464403	-3.552643	-0.142919
C	4.328404	3.652331	0.929327
H	4.254033	2.962723	1.765079
C	1.126160	-2.839676	-0.142885
C	4.185796	-0.625393	-0.509826
H	5.031446	-1.276606	-0.672510
C	2.454740	-2.415261	-0.237394
C	0.607668	4.211085	0.119510
H	1.261917	5.065447	0.207442
C	2.385625	2.462795	-0.141446
C	4.434362	-3.589510	0.781666
H	4.343723	-2.934961	1.643601
C	5.313440	4.645917	0.948295
H	5.982875	4.710688	1.797536
C	-2.863602	1.049122	-0.170125
C	5.447248	-4.554596	0.759561
H	6.121551	-4.632816	1.603798
C	-4.593705	-5.412982	-1.237637
H	-4.717474	-6.081550	-2.083322
C	-4.323926	-3.711861	0.949227
H	-4.220823	-3.050749	1.804721
C	-0.632468	-4.241776	-0.011009
H	-1.283558	-5.099429	0.067622
C	-3.617532	-4.423355	-1.236806
H	-2.963028	-4.314196	-2.096509
C	-5.439468	4.486208	1.103330
H	-6.108055	4.568503	1.954028
C	-4.435256	3.525929	1.064981
H	-4.314616	2.841223	1.899226
C	0.727996	-4.221911	-0.037578
H	1.406470	-5.060120	0.015132

C	-5.603236	5.376181	0.030549
C	-2.832680	-1.152164	-0.204509
C	-4.748299	5.292147	-1.075923
H	-4.853780	5.962034	-1.920702
C	-3.739783	4.322313	-1.095100
H	-3.080461	4.259875	-1.955912
C	4.671947	-5.274102	-1.421620
H	4.783473	-5.935774	-2.274399
C	-5.308872	-4.705479	0.967904
H	-5.949481	-4.798659	1.836508
C	-5.445968	-5.561445	-0.132483
C	7.457949	-6.558304	0.569248
H	8.060769	-5.654460	0.727100
H	8.107099	-7.374810	0.250404
H	6.961192	-6.833954	1.508611
C	-7.267001	-6.766465	0.859082
H	-6.728514	-7.023298	1.780604
H	-7.903710	-7.602661	0.567349
H	-7.889247	-5.879397	1.035486
C	-6.837164	7.214556	-0.890978
H	-5.959440	7.855546	-1.045738
H	-7.681642	7.828008	-0.574312
H	-7.088499	6.707127	-1.831483
C	7.266307	6.712284	0.843269
H	6.759042	6.937136	1.790518
H	7.892627	7.558726	0.558663
H	7.894454	5.820700	0.968683
N	0.017734	-0.046145	1.788956
O	0.038734	-0.067129	2.967162

References

1. SMART, SAINT and XPREP; Siemens Analytical X-ray Instruments Inc.: Madison, Wisconsin, USA, 1995.
2. (a) G. M. Sheldrick, *SHELXS-2014*; University of Gottingen, Germany. (b) L. J. Farrugia, ORTEP-3 for Windows - a version of ORTEP-III with a Graphical User Interface (GUI). *J. Appl. Crystallogr.* 1997, **30**, 565–565.
3. Gaussian 16, Revision A.03, M. J. Frisch, G. W. Trucks, H. B. Schlegel, G. E. Scuseria, M. A. Robb, J. R. Cheeseman, G. Scalmani, V. Barone, G. A. Petersson, H. Nakatsuji, X. Li, M. Caricato, A. V. Marenich, J. Bloino, B. G. Janesko, R. Gomperts, B. Mennucci, H. P. Hratchian, J. V. Ortiz, A. F. Izmaylov, J. L. Sonnenberg, D. Williams-

Young, F. Ding, F. Lipparini, F. Egidi, J. Goings, B. Peng, A. Petrone, T. Henderson, D. Ranasinghe, V. G. Zakrzewski, J. Gao, N. Rega, G. Zheng, W. Liang, M. Hada, M. Ehara, K. Toyota, R. Fukuda, J. Hasegawa, M. Ishida, T. Nakajima, Y. Honda, S139 O. Kitao, H. Nakai, T. Vreven, K. Throssell, J. A. Montgomery, Jr., J. E. Peralta, F. Ogliaro, M. J. Bearpark, J. J. Heyd, E. N. Brothers, K. N. Kudin, V. N. Staroverov, T. A. Keith, R. Kobayashi, J. Normand, K. Raghavachari, A. P. Rendell, J. C. Burant, S. S. Iyengar, J. Tomasi, M. Cossi, J. M. Millam, M. Klene, C. Adamo, R. Cammi, J. W. Ochterski, R. L. Martin, K. Morokuma, O. Farkas, J. B. Foresman, and D. J. Fox, Gaussian, Inc., Wallingford CT, 2016.

4. A. D. Becke, *J. chem. phys.* 1992, **96**, 2155-2160.
5. R. H. W. J. Ditchfield, W. J. Hehre and J. A. Pople, *J. chem. phys.* 1971, **54**, 724-728.
6. F. T. Bonner and Y. H. Ko, *Inorg. Chem.* 1992, **31**, 2514–2519.